NASA Technical Memorandum 109182

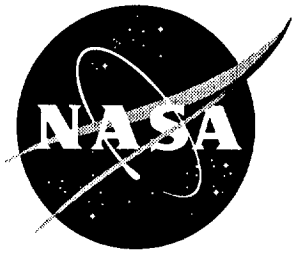

Dynamic Response Tests of Inertial and Optical Wind-Tunnel Model Attitude Measurement Devices

R. D. Buehrle
Langley Research Center, Hampton, Virginia

C. P. Young, Jr.
North Carolina State University, Raleigh, North Carolina

A. W. Burner, J. S. Tripp, P. Tcheng, T. D. Finley, and T. G. Popernack, Jr.
Langley Research Center, Hampton, Virginia

February 1995

National Aeronautics and
Space Administration
Langley Research Center
Hampton, Virginia 23681-0001

Table of Contents

List of Tables and Figures

Summary

Results are presented for an experimental study of the response of inertial and optical wind-tunnel model attitude measurement systems in a wind-off simulated dynamic environment. This study is part of an ongoing activity at the NASA Langley Research Center to develop high accuracy, advanced model attitude measurement systems that can be used in a dynamic wind-tunnel environment. This activity was prompted by the inertial model attitude sensor response observed during high levels of model vibration. The inertial sensors cannot distinguish between the gravitational acceleration and centrifugal accelerations associated with wind-tunnel model system vibration which results in a model attitude measurement bias error. Significant bias errors in model attitude measurement were found for the measurement using the inertial device during wind-off dynamic testing of a model system. The amount of bias present during wind-tunnel tests will depend on the amplitudes of the model dynamic response and the modal characteristics of the model system. Correction models were developed and used to predict the vibration-induced bias errors for the inertial device. A correction model based on the measured vibration amplitudes and modal characteristics of the model system predicts the bias error to a high degree of accuracy for the vibration modes characterized in the simulated dynamic environment. The optical system results were uncorrupted by model vibration in the laboratory setup. The optical model attitude measurement system and correction methods for the inertial model attitude measurement system are to be validated during actual wind-tunnel tests.

Introduction

The predominant instrumentation used to measure model attitude or angle of attack (AOA) in wind-tunnel testing at NASA Langley Research Center (LaRC) is the servo-accelerometer device described in reference 1. For quasi-static conditions, this inertial sensor provides a model attitude measurement with respect to the local gravity field to an accuracy of ±0.01° over a range of ±20°. However, during wind-tunnel testing, dynamic pitching and yawing motion of the model creates centrifugal acceleration which is sensed by the onboard inertial AOA device and results in a bias error in the model attitude measurement. The amount of bias present during wind-tunnel tests will depend on the amplitudes of the model dynamic response and the modal characteristics of the model system. The problem of the inertial device sensitivity to model vibrations is briefly discussed in reference 1.

The National Transonic Facility (NTF) [2] is a transonic wind-tunnel located at NASA LaRC which has the capability for testing models at Reynolds number up to 140 million at Mach 1 and dynamic pressure up to 7000 pounds per square foot. Severe model vibrations have been encountered on a number of models since the tunnel began operation. References 3 through 6 document studies of model and model support vibrations in the facility. Reference 7 documents results of an experimental study conducted in 1993 at the NTF to study the inertial AOA sensor response to a simulated dynamic environment. The experimental study [7] clearly established that AOA bias error is due to centrifugal forces associated with model vibration. During wind-off dynamic tests, bias errors over an order of magnitude greater than the desired device accuracy of 0.01 degree were measured. The bias error was found to be dependent on the vibration mode and amplitude. The study revealed the complexity of the

problem when multiple vibration modes were present involving both pitch and yaw motions. A first-order correction model was devised from the problem physics which gave good estimates of bias error when compared with test results.

Although the reference 7 study was conducted at the NTF, the AOA measurement error due to model dynamics is not unique to this facility or to cryogenic facilities. The problem exists anytime model attitude is being measured by an inertial device in the presence of significant model system vibrations. The amount of error in the inertial model attitude measurement is dependent on the model system dynamics (i.e., will vary for each model system) and is very difficult to quantify during actual wind-tunnel tests.

Inertial sensors have other problems besides the possible bias errors caused by model dynamics. These problems include: (1) requirements for special handling due to their fragile nature, (2) requirements for multiple accelerometers for the measurement of pitch and roll, and (3) space and wiring requirements in the model fuselage. For these reasons (in addition to the possibility of dynamic bias errors), alternative methods for measuring AOA at NTF (and other tunnels) have been sought. Much of the interest has been in optical techniques which are generally assumed to be immune from the dynamic problems inherent in inertial devices. However, even though an optical technique may not be theoretically corrupted by model dynamics, experimental implementation may lead to errors due to dynamics caused by such things as variations in irradiance, camera/laser mounting system vibrations, and aliasing. Therefore, dynamic tests must be conducted on any AOA measurement technique, including optical techniques.

This report describes an experimental study of the response of inertial and optical model attitude measurement devices to a wind-off dynamic environment. The inertial and optical measurement techniques are described and problems associated with the implementation of these techniques in a dynamic wind-tunnel environment are discussed. The measurement results for each of the devices are presented for a simulated dynamic environment under wind-off conditions.

Symbols List

AOA	angle of attack
A_{fil}	filtered AOA signal from inertial device
A_r	peak acceleration for r^{th} vibration mode
$a_n(t)$	time dependent normal acceleration
$a_t(t)$	time dependent tangential acceleration
$a_x(t)$	time dependent longitudinal acceleration
$A_{unf}(t)$	time dependent unfiltered AOA signal
g	gravitational constant
Hz	Hertz
m	number of included modes

q(t)	time dependent inertial AOA output
r	current mode number
S_{qq}	power spectrum of q(t)
S_{yy}	power spectrum of y(t)
S_{qy}	cross spectrum of q(t) and y(t)
t	time in seconds
$v_r(t)$	time dependent velocity for r^{th} mode
V_r	peak velocity for r^{th} mode
x(t)	time dependent lateral motion (via balance or accelerometer output)
y(t)	integral-square of x(t)
$y_r(t)$	time dependent displacement for r^{th} mode
Y_r	peak displacement for r^{th} mode
$\frac{d}{dt}$	derivative with respect to time
α	angle of attack
Γ_{qy}	cross-spectral coherence function for q(t) and y(t)
ρ_r	effective radius of r^{th} vibration mode
ω_r	circular frequency of r^{th} mode
°	degrees

Model Attitude Measurement Systems

Inertial System

The inertial AOA package used at LaRC [1] to sense the attitude of the model is shown installed in the nose of a test model in figure 1. The AOA package uses a servo-accelerometer with its sensitive axis parallel with the longitudinal axis of the model. For quasi-static conditions, this sensor provides a model attitude measurement with respect to the local gravity field to an accuracy of ±0.01° over a range of ±20°. Most wind-tunnels use a cantilever arm (sting) to support the model. The model mounted at the end of the sting experiences dynamic oscillations due to unsteady flows that induce centrifugal accelerations on the inertial AOA package and result in angle of attack measurement errors.

Physics of Problem. The physics of the problem are studied by considering the response of a single yaw mode as simple harmonic motion as depicted in figure 2. For the system shown

with natural frequency of oscillation, ω_r, the AOA package displacement, $y_r(t)$, and velocity, $v_r(t)$, can be written:

$$y_r(t) = Y_r \sin(\omega_r t) \tag{1}$$

$$v_r(t) = \frac{dy_r}{dt} = V_r \cos(\omega_r t); \quad \text{where } V_r = Y_r \omega_r \tag{2}$$

The corresponding tangential and normal acceleration components, a_t and a_n, are:

$$a_t(t) = \frac{dv_r}{dt} = A_r \sin(\omega_r t); \quad \text{where } A_r = -Y_r \omega_r{}^2 \tag{3}$$

$$a_n(t) = \frac{v_r{}^2(t)}{\rho_r} = \frac{V_r^2}{\rho_r}\cos^2(\omega_r(t)) = \frac{V_r^2}{2\rho_r}(1+\cos(2\omega_r t)) \tag{4}$$

Rewriting equation (4) in terms of peak acceleration gives

$$a_n(t) = \frac{A_r{}^2}{2\omega_r{}^2 \rho_r}(1+\cos(2\omega_r t)) \tag{5}$$

The vibration-induced normal acceleration results in the AOA package sensing a centrifugal acceleration coincident with its sensitive axis (i.e., the longitudinal axis of the model). The AOA package output prior to filtering becomes:

$$A_{unf}(t) = g\sin\alpha - \frac{V_r^2}{2\rho_r}(1+\cos(2\omega_r t)) + a_x(t) \tag{6}$$

The first term on the right-hand side of the equation is the gravitational acceleration due to the model attitude, α, relative to the local vertical. The second term is the centrifugal acceleration (from equation (4)) caused by the model yaw motion. Accelerations resulting from flow-induced longitudinal model vibrations (typically high frequency) are represented by the third term. To obtain the mean angle, the AOA signal is lowpass filtered (0.4 Hz cut-off frequency).

$$A_{fil} \approx g\sin\alpha - \frac{V_r^2}{2\rho_r} \tag{7}$$

It is important to note that the model vibration causes a bias error in the model attitude measurement that cannot be removed by filtering or data averaging.

Model pitch vibration causes a similar bias error term, where the tangential velocity is acting in the pitch plane. If the vibration response is composed of multiple yaw and pitch modes, the total bias error will be a linear summation of the error contributions for the m modes.

$$A_{fil} \approx g\sin\alpha - \sum_{r=1}^{m} \frac{V_r^2}{2\rho_r} \tag{8}$$

Or, in terms of the peak acceleration, from equation (5),

$$A_{fil} \approx g\sin\alpha - \sum_{r=1}^{m} \frac{A_r^2}{2\omega_r^2 \rho_r} \tag{9}$$

The above discussion is based on the case of continuous sinusoidal model motion. In the wind-tunnel, the data is non-stationary and random in nature. This results in a time varying bias error that is dependent on the number of modes participating and the amplitudes of motion for those modes (i.e., $V_r(t), A_r(t), A_{fil}(t)$).

Bias Error Correction. Several methods have been proposed to correct for this bias error using measured tangential accelerations at the AOA sensor location due to model yaw and pitch motion. One method is to measure the natural frequencies from the frequency spectra of the tangential accelerations and then determine the bias magnitudes by measuring the magnitude of the second harmonic components from the frequency spectrum of the unfiltered AOA signal (see equation (6)). This technique may be difficult to implement due to the participation of multiple modes and the required data accuracy to measure the small magnitudes at the second harmonic frequency. Young et. al. [7] determine the natural frequencies, ω_r, and corresponding peak acceleration magnitudes, A_r, from the frequency spectra of the yaw and pitch acceleration measurements. The bias error is then calculated from the second term of equation (9). The vibration mode effective radius, ρ_r, was estimated from sinusoidal input-output data taken during wind-off ground vibration tests and later confirmed with measured mode shapes. Both techniques use frequency domain signal processing which is suitable for the stationary data observed in the wind-off tests but is questionable when evaluating the non-stationary data observed during wind-tunnel testing.

A third bias correction technique was developed and used at the National Aerospace Laboratory (NLR) in the Netherlands. This technique was developed for one vibration mode in each the yaw and pitch plane. Two additional accelerometers are used to measure the tangential accelerations due to the yaw and pitch motion of the model. The tangential accelerations are integrated to obtain velocity, squared, and divided by a scale factor to compensate for the effective radius of the vibration mode. This signal is then added to the unfiltered AOA output to cancel the second term of equation (6). The corrected signal is then lowpass filtered to obtain the corrected mean AOA measurement. The mode radius in the yaw and pitch plane is determined by tuning a potentiometer while manually exciting the

model in the yaw and pitch plane, respectively. This technique does not address the case where multiple yaw and pitch vibration modes are present.

During wind-off dynamic testing of a model system [7], significant vibration-induced bias errors were found for multiple modes. The "modal correction method" is being developed to extend the time domain technique used at NLR to compensate for multiple yaw and pitch vibration modes. This technique estimates the mode effective radii using measured modal properties of the model system. Accelerations measured tangent to the AOA package sensitive axis are band-pass filtered to isolate individual modes. The filtered signal is then integrated, squared, and divided by the corresponding mode effective radius to determine the bias error for a particular mode (second term of equation (6)). To compensate for multiple modes, a linear superposition of the individual mode effects is used to estimate the total bias error as a function of time. The estimated total bias error is then added to the AOA output prior to filtering. This corrected signal is lowpass filtered to obtain the corrected mean AOA measurement.

The mode radii are estimated by assuming the fuselage moves as a rigid body and using a least squares fit of the fuselage mode shape coefficients to determine an effective point of rotation for each mode. A vibration mode's effective radius is estimated as the distance from the mode's point of rotation to the inertial AOA sensor location in the model fuselage. This may be more easily understood by examining the measured mode shapes that are shown in figures 3 and 4. Figure 3 shows the 9.0 Hz model/sting bending mode in the yaw plane with a projected point of rotation aft of the model fuselage. Figure 4 shows the 29.8 Hz model yaw mode with a projected point of rotation forward of the AOA package. For the 29.8 Hz mode, the effective radius is negative. Previously, it was assumed that the centrifugal accelerations for all modes would act in the same direction, i.e., the point of rotation was always aft of the AOA package. However, this data indicated that the dynamically-induced errors could be positive or negative dependent on the mode shape (mode effective radius).

The rigid body assumption used in the mode radius estimation appears to be satisfactory for the low frequency (< 50 Hz) modes that are being evaluated. A second assumption is that the mode shapes do not change significantly under the wind-tunnel test conditions. This enables wind-off estimates of the mode effective radii to be used for on-line correction of the model attitude measurement during wind-tunnel testing. Further work is required to validate this assumption.

Another method under development uses time and frequency domain analyses to estimate and correct for the dynamic bias error. This proposed correction method is the subject of a separate paper being developed by one of the co-authors. The main difference between this method and the modal correction method is that the modal radius is estimated by a least squares fit of the integral-squared yaw (or pitch) moment to the dynamic AOA output. This requires a longer data record initially (≥ 10 seconds) to obtain a good estimate of the mode radius. The proposed time and frequency domain bias error correction algorithm proceeds as follows: (1) Acquire dynamic time-series records of inertial AOA output and denote as q(t); (2) Acquire dynamic time series records of lateral motion containing angular acceleration via balance output or accelerometer output and remove the mean value (denote as x(t));

(3) Numerically integrate x(t), square, and denote by y(t); (4) Compute power spectra S_{qq} and S_{yy}, cross-spectrum, S_{qy}, and cross-spectral coherence function Γ_{qy}; (5) Inspect Γ_{qy} for spectral correlation within the AOA filter passband and identify the corresponding modal frequencies (denote as ω_r); (6) Estimate radius, ρ_r, corresponding to each mode; (7) Band-pass filter lateral motion signal x(t) about modal frequency ω_r and denote as $x_L(t)$; (8) Low-pass filter dynamic AOA signal and denote by $q_L(t)$; (9) Numerically integrate and square $x_L(t)$ and denote by $y_L(t)$; (10) Correct inertial AOA output, $q_L(t) - y_L(t) / \rho_r$, and lowpass filter the result; (11) Repeat for each mode.

A sensitive correlation test between the time series q(t) and y(t) is provided by the cross spectral density coherence function, defined as follows:

$$\Gamma_{qy}(\omega) = \frac{\left|S_{qy}(\omega)\right|}{\sqrt{S_{qq}(\omega) \times S_{yy}(\omega)}} \tag{10}$$

where $S_{qq}(\omega)$ and $S_{yy}(\omega)$ are the power spectra of q(t) and y(t), respectively, and $S_{qy}(\omega)$ is the cross spectrum. Correlated spectral components common to both $S_{qq}(\omega)$ and $S_{yy}(\omega)$ appear in $\Gamma_{qy}(\omega)$. Other spectral components common to $S_{qq}(\omega)$ and $S_{yy}(\omega)$ which are not phase coherent, i.e., unsynchronized, tend to be removed from $S_{qy}(\omega)$ by averaging and cancelled by normalization and do not appear in $\Gamma_{qy}(\omega)$. The coherence function and cross spectrum thus provide a means of detecting and quantifying AOA bias errors due to angular oscillation.

Optical System

A number of optical techniques have been investigated for measuring AOA [8-11], but none of these appear practical for both air and cryogenic (nitrogen) operations such as the NTF. Some of the problems with these and other optical techniques are that lasers are often used as light sources which require special considerations for packaging in a harsh wind-tunnel environment (especially a cryogenic high pressure environment such as the NTF). In addition, special sensors (some requiring wiring) may need to be placed in the model fuselage. Some of these devices may require windows in the fuselage which need special protection during model preparation. Another problem common to most of the optical techniques (including the video technique discussed here) is that fog in the test section may attenuate light to the point where the optical angle measuring system may not work at all. The onboard inertial sensor, however, is not affected by tunnel fog. Tunnel fog is not an operational problem in the NTF but may be encountered in other wind-tunnels.

Recent success at NTF in measuring wing twist in both air and cryogenic runs led to the question of whether or not a similar technique could be used to measure model AOA at the facility. At NTF, wing twist is determined optically from photogrammetric measurements made on digital video images. The technique is based upon a single camera photogrammetric determination of two dimensional coordinates with a fixed (and known) third

dimensional coordinate. The wing twist is found from a conformal transformation between flow and no-flow 2-D coordinates in the plane of rotation.

Since reduced data are not available in "real-time", the current wing twist technique was initially not deemed suitable as the primary means of determining AOA. However, it was thought that additional AOA data from such a technique (especially data at dynamic conditions) might aid in the analysis of the dynamic bias error problem associated with inertial sensors. For this reason, and to gain initial wind-tunnel experience with the technique for measuring AOA, data were taken for a number of runs over several days at both air and cryogenic conditions. Instead of using targets on the fuselage (in a manner similar to that used for wing twist), a fortuitous glint near the top of the fuselage caused by a specular reflection from one of the test section lights was used as a line source from which the slope and intercept could be computed and AOA determined. It was determined from this limited data set that if the onboard accelerometer was used for no-flow calibration at a particular tunnel temperature, then the AOA could be measured with flow to 0.02° root mean square (rms) in air mode and 0.05° rms in cryogenic mode when compared to the onboard accelerometer. Worst case disagreement with the onboard inertial sensor was 0.2 degrees. It was not determined during these tests how much of the disagreement was due to model dynamics causing bias errors in the inertial sensor measurements and how much of the disagreement was due to the video angle of attack measurement. Given the potential advantages of the video method, the results were considered encouraging enough to continue development and testing of the technique.

Major advantages of the video angle measurement method compared to other optical techniques are that no laser is required since existing test section lights are used to illuminate the model, and no sensor is required in the model fuselage. In addition, for NTF, many of the operational problems associated with the packaging of instrumentation in a cryogenic high pressure environment, window frosting and equipment survivability have already been addressed during the development of the wing twist method. The difficulty of these operational problems should not be underestimated. Some of the solutions to these problems are not satisfactory, even after eight years of tunnel testing with video systems.

One disadvantage of the image-based video technique is that lighting requirements for AOA may differ from the lighting requirements for general model surveillance. For very critical surveillance, the Test Engineer may find it necessary to re-adjust the test section lighting which might invalidate the video calibration or may even cause the video technique to be unable to reduce data at all. Another concern with the video method is the potential sensitivity of the technique to the location of the line to be measured on the image plane. This sensitivity to line image location may be difficult to completely compensate by calibration. Another disadvantage is that the technique does not function as an angle transducer to produce a voltage output proportional to angle as is common to most of the other optical techniques and inertial sensors. Wind-tunnel data acquisition systems are generally set up to handle such transducers in a standard manner. To measure angle with the video technique, computations on the gray scale of digital images are required. These computations, while amenable to automation for a fixed geometry and high contrast, make it difficult to automate the process to include variable geometry, especially if high contrast

cannot be maintained. In addition, camera alignment stability, practical in-place facility calibration, and various assumptions made for the single camera photogrammetric solution are all issues which have not been fully addressed. Further laboratory and tunnel tests are necessary to more completely characterize and develop the video technique before it is suitable for routine use.

EXPERIMENTAL TEST SETUP AND PROCEDURES

The test setup is shown in figure 5. Inertial and optical systems were used to measure the attitude of a cantilevered model system during dynamic tests under wind-off conditions.

Instrumentation

The model system was installed in a model assembly bay at the NTF as shown in figure 5. The mounting consisted of a "rigidly" supported cantilever (sting) that is positioned by a pitch-roll-translation mechanism. The model is attached to the sting through a six component strain gage balance.

The model was instrumented with an inertial AOA package [1] maintained at a constant temperature of 160°F. The signal conditioner for the AOA package provides both an unfiltered (0–300 Hz bandwidth) signal and a filtered (0–0.4 Hz bandwidth) signal. Two miniature accelerometers were installed on the face of the AOA package to measure the accelerations tangent to the sensitive axis of the AOA sensor in the yaw and pitch planes of the model. In addition, four accelerometers were mounted external to the model fuselage to measure model yaw and pitch motion.

An electrodynamic shaker was used to excite the model through a single point force linkage as shown in figure 6. The excitation was input in the pitch and yaw planes at the model fuselage hardpoints, approximately 36 inches forward of the balance moment center. Sine, modulated sine, and band-limited (5–60 Hz) random shaker inputs were used.

Data Acquisition Systems

Dynamic Signal Analyzer. A Hewlett Packard model 3566A dynamic signal analyzer (see figure 7) was used to provide the shaker stimulus and perform on-line time and frequency domain signal analysis. The 16 channel signal analyzer was used to monitor and record the shaker force input, model force balance outputs, AOA filtered (static) and unfiltered (dynamic) outputs, and model accelerations. This system was also used to monitor the model yaw and pitch moments which established the dynamic test conditions for acquiring model attitude measurements.

Optical System. The optical technique used to determine model attitude for these tests is based upon the recording and analysis of digitized video images. Figures 8 and 9 show the optical system setup. A video signal from a standard RS-170 solid state camera with 752 horizontal X 240 vertical pixels per field is routed to a frame grabber controlled by a 486-66 MHz PC which records video fields every 1/60 second until the grabber memory

(4 Mbytes) is full. Even and odd fields are stored sequentially. The contents of the grabber memory are then stored on hard disc in a temporary file which is overwritten each time an angle measurement is made. For these tests the sensor field integration time was set to 1 milli-second. A 35 mm focal length lens set to an F-number of 4 was used for imaging. The video image is windowed to about 1/3 of full field (752H X 92V pixels) so that 60 fields are recorded in 1 second. For selected points, the window of interest was reduced to 752H X 20V pixels in order to record ~ 4.6 seconds of data. This reduced windowing was practical since the nominal pitch angle for many of the points was near 0° and was fixed for a given run. Data recording was initiated by contact closure to the frame grabber which simultaneously triggered the Data Acquisition System (DAS) described in the next section.

A glint near the top of the fuselage was used as a line object to determine AOA. This glint was formed from a specular reflection from one of the overhead lights. Vertical line centroids are computed every 20 columns. The pixel coordinates are converted to image plane coordinates in units of length from the known horizontal and vertical pixel spacing. The image plane coordinates for the glint are converted to X, Z coordinates based on the collinearity relation of photogrammetry. The collinearity equation relates the 3D object coordinates to the 2D image plane coordinates. If one of the object coordinates is known then image plane coordinates from a single camera can be used to determine the other two coordinates. For the case of a model which pitches in the vertical X, Z plane, the Y coordinate is assumed known. The slope angle and standard deviation of slope angle are then computed from the X, Z object coordinates of the glint. The slope angle and standard deviation for the line computations for each of the 60 fields is output to a file for each point along with the trigger time, y-intercept, and standard deviation of y-intercept. In addition, the mean angle and intercept along with their standard deviations are appended to a log file containing all the points. The standard deviations in the log file, computed from the 60 values of angle and intercept, indicate variability during data taking and differ from the line standard deviations (indicating deviation from a straight line) as output to the individual point files. The standard deviation of y-intercept in the log file is useful as a measure of motion in the pitch plane during data taking. Angle plots as a function of time and the mean and standard deviation of the 60 fields are displayed on the computer monitor after each point to ensure proper operation. Data recording was programmed with a script file for automatic acquisition upon contact closure.

The initial pre-test calibration procedure for the video optical technique consists of determining various camera parameters necessary to convert from pixels to corrected image plane coordinates. Techniques for determining these parameters are discussed in references 12 and 13. The need for extensive camera calibration is lessened considerably by on-line angle calibrations using the onboard angle sensor for reference under no-flow conditions. For the preparation bay test, nominal values were used for the camera parameters based on previous calibrations.

The next calibration step at the start of the test is the determination of the camera's pointing angles and location in the tunnel coordinate system. This would normally be accomplished by space resection on a known target field since alignment options in the tunnel test section are limited. Instead, for these tests the camera could be aligned to be parallel to the Y axis

and the location of the cameras front perspective center was estimated from direct measurements. The camera was located 56 inches from the center of the fuselage. Normally the final calibration step is to run a no-flow pitch sweep over the range of angles of interest in which the onboard inertial sensor is used for angle calibration at each tunnel temperature. For the preparation bay tests, only differences from the no-load angle were of interest so that no angle calibrations were required.

Data Acquisition System. The Data Acquisition System (DAS), shown in figure 10, is a 12 channel digital data acquisition system with 16-bit resolution. For the tests, data were recorded at a rate of 800 samples per second per channel. Recorded channels included the unfiltered and filtered inertial AOA output, the auxiliary yaw and pitch accelerometer outputs, the six unfiltered balance components, the shaker excitation function, and an auxiliary optical AOA sensor output.

Test Procedure

The model was set at a prescribed angle of attack under static conditions. The model system natural frequencies were identified using sine sweep excitation of the model in the pitch and yaw planes. For each natural frequency of interest, a sinusoidal forced response test was conducted by controlling the shaker input amplitude to provide a defined peak-to-peak pitch or yaw moment on the model force balance. The control test variables were pitch moment for modes that had predominantly pitch motion, and yaw moment for modes that had predominantly yaw motion. Inertial and optical systems were used to measure the model attitude for a series of moment amplitude levels for sinusoidal excitation at a prescribed natural frequency of the model system. Sinusoidal forced response tests were conducted with the model set at pitch angles of 0°, 4.3° and 6°.

In addition to the sinusoidal forced response tests, the model attitude was measured for modulated sine and random excitation tests. The modulated sine and random excitations/responses are more representative of the model dynamics observed in actual wind-tunnel tests. The majority of the modulated sine tests were conducted with a 0.25 Hz modulation of the first natural frequency in the pitch and yaw planes. The random excitation was only evaluated in the pitch plane for the model at a nominal angle of 0°. In each case, the inertial and optical systems were used to measure the model attitude for a series of moment amplitude levels.

Discussion of Test Results

Inertial System

Modal Correction Technique. Attempts were made to excite three natural vibration modes in each of the yaw and pitch planes of the model system. The modes of interest were determined from previous modal surveys of the model system and are listed in Table 1. The slight shift in mode frequencies indicated for mode 1 were attributed to differences in the assembly bay test setup (i.e., shaker attachment/alignment; boundary conditions to

accommodate model angle change). Measurements taken during previous wind-tunnel tests indicated that the two primary modes being excited were at approximately 8–10 Hz and 28–30 Hz [6] in the yaw plane. The radius for a vibration mode was determined using a least squares fit of the modal deformations on the model fuselage to project the rigid body motion of the fuselage to a point of rotation (see figures 3 and 4). The vibration mode effective radius is then estimated as the distance from the mode rotation point to the inertial AOA sensor location in the model fuselage. These predictions indicated that the radius may be positive or negative dependent on the vibration mode shape. For the case were the radius is positive, the point of rotation for the vibration mode is ahead of the AOA package. The significance of the sign of the radius is that the bias error effect may be positive or negative dependent upon the vibration mode being excited. This is demonstrated by the response for the yaw plane modes shown in figures 11 through 13. For the first two yaw modes (9.8 and 19.5 Hz), the indicated model angle change is negative when the model is being driven with sinusoidal excitation at the mode natural frequency and then returns to its nominal angle when the shaker system is shutoff. The third yaw mode (29.8 Hz), which has a negative radius value, shows an indicated positive angle change when the model is being driven with sinusoidal excitation at the mode natural frequency and then returns to its nominal angle when the shaker system is shutoff. The excitation system was adequate to show the above trends; however, the higher frequency modes (>10 Hz) were difficult to drive and only the first mode in each the yaw and pitch planes were excited to levels that showed significant shifts in the indicated model attitude from the onboard inertial AOA package. Difficulty in driving the higher frequency modes is attributed to the rigid backstop support in the model assembly bay. During previous wind-tunnel tests [6], the model coupled with the model support structure resulting in high dynamic yaw moments with energy in the 28–30 Hz band. This points out the need to do modal testing with the model installed in the tunnel.

Table 1
Model System Vibration Mode Characteristics

Mode No.	Natural Frequency (Hz)	Effective Radius[1] (inches)	Mode Description
1	8.8 to 9.8 [2]	31.0	Sting First Bending in Yaw
2	9.2	30.2	Sting First Bending in Pitch
3	19.5	0.18	Model Yawing on Balance with Sting First Bending
4	20.3	-1.08	Model Pitching on Balance with Sting First Bending
5	29.8	-7.14	Model Yawing on Balance with Sting Second Bending
6	34.2	-7.65	Model Pitching on Balance with Sting Second Bending

Note: (1) The effective radii from the point of rotation for a mode to the AOA sensor location are based on data from 7/93 modal survey. (2) Slight frequency changes were measured for different model setups (i.e., pitch angles of 0, 4.3, and 6 degrees).

The results of sinusoidal excitation tests (model at nominal angle of 0°) for the first mode in the yaw and pitch plane is shown in figures 14 and 15. For a set excitation level, time domain data were acquired and stored using the Hewlett Packard signal analyzer. These data were transferred to a personal computer where a software routine, written as an M-file in the MATLAB [14] language, was used to estimate the bias error in the inertial device. The yaw and pitch plane accelerations were bandpass filtered, integrated to obtain velocity, squared, divided by the mode effective radii, and scaled to obtain the equivalent angle change in degrees. The estimated bias error is in good agreement with the indicated mean angle change measured with the onboard inertial AOA sensor. If the estimated bias error is subtracted from the indicated model angle, the error would be reduced from a maximum of -0.146° to -0.009° for the first mode in the yaw plane (y) and from -0.175° to -0.006° in the pitch plane (z). These corrections are within the AOA accuracy requirement of 0.01°. Similar results were obtained for the sinusoidal input tests with the model at nominal angles of 4.3° and 6°.

In addition to the sinusoidal tests, the bias error was examined for modulated sine and random inputs. Figure 16 shows the estimated and measured bias error as a function of time for a 9.2 Hz pitch excitation with a 0.25 Hz modulation. Excellent agreement is obtained with the difference between the estimated and measured bias being less than 0.005°. Modulated sine tests were conducted for the first mode in each the y and z axes at several excitation amplitude levels and consistent results were obtained between the measured and predicted bias errors for all cases. In the pitch plane, two levels of random excitation were input to the model. An eight second record of the inertial AOA sensor response for the highest level random excitation is shown in figure 17. The random response measured by the vertical (pitch plane) accelerometer on the face of the AOA package was composed of primarily 9.2 Hz response. The bias estimate based on only the 9.2 Hz mode contribution is also shown in figure 17. Again, the estimated and measured bias are in very good agreement.

Time and Frequency Domain Analysis. The utility of spectral techniques in identifying dynamic AOA data records corrupted by angular motion is illustrated in the following data set obtained during yaw excitation. The model is excited in yaw at 5300 inch-pound amplitude at 9.75 Hz, modulated at 0.3 Hz. Figure 18 illustrates a 70 second record of the filtered AOA time series and the corresponding integral-squared yawing moment. Figure 19 depicts their corresponding power spectra. The apparent good agreement at 0.3 Hz seen both in the time series and in the power spectra is corroborated by the well defined 0.3 Hz peak in the cross spectral coherence shown in figure 20, and by the absence of significant energy below 0.3 Hz in both power spectra. AOA bias correction to better than 0.01° was obtained in the first third of the record.

For comparison, the integral-squared y-axis accelerometer time series and its power spectrum appear in figures 21 and 22. Note that the time series agreement with AOA is poor in the latter third of the record, and note the presence of significant power spectral energy from 0 to 0.3 Hz in the integral-squared y-axis accelerometer record, which is absent in the AOA power spectrum. The cross spectral coherence seen in figure 23 shows no correlation below 0.3 Hz and less pronounced correlation at 0.3 Hz than for yaw. Since the low

frequency content of the record is uncorrelated with AOA, poor correction is likely using y-axis accelerometer data. This is confirmed in the latter third of the time series of figure 21 where AOA bias correction to within 0.1° cannot be obtained. Note that the correction will be poor in this time segment even if the modal radius is known from prior testing because of the wave shape disagreement.

Single mode bias correction using the previously described time and frequency domain procedure was applied to the modulated sine data sets for pitch excitation. Its efficacy was compared using the integral-squared time series of pitching moment, normal force, and the z-axis accelerometer. Selected results are tabulated in Table 2 showing the time and duration of the corrected time series, the source of the integral-squared correction, the mean and standard deviation of the filtered uncorrected AOA, the bias error estimated by the regression, the mean of the corrected AOA, and the standard error of the regression.

Table 2
Estimated Bias Error with Pitch Excitation
(Unexcited Data Zero, AOA = -0.290°)

Record Segment (Sec)	Correction Source	Mean Filtered AOA (Deg)	Standard Deviation Filtered AOA (Deg)	Bias Estimate (Deg)	Mean Corrected AOA (Deg)	Standard Error (Deg)
15–85	Pitch	-0.337	0.048	-0.064	-0.273	0.014
20–40	Pitch	-0.332	0.046	-0.059	-0.273	0.006
40–60	Pitch	-0.335	0.046	-0.067	-0.268	0.005
20–40	Normal	-0.332	0.046	-0.095	-0.237	0.030
20–40	Z Accel.	-0.332	0.046	-0.064	-0.268	0.011

Figure 24 shows residuals obtained from the AOA and integral-squared pitch time series over the 15 to 85 second time interval. The 0.014 degree standard error represents a 71 percent reduction below the 0.048 degree filtered AOA standard deviation. Note that the 0.06 degree impulse at the time of 70 seconds due to a corresponding disturbance in the filtered AOA contributes a significant portion of the variance over the 70 second interval. Figure 25 shows residuals over the 20 to 40 second time interval. The 0.0057° standard error of the regression over the 20 second interval shown in figure 25 accounts for 88 percent of the 0.046° filtered AOA standard deviation over the same interval.

Less accurate regression corrections are obtained from the integral-squared normal force and z-axis accelerometer data records, both of which contain spectral content below the modulation frequency which is uncorrelated with the AOA time series. These and other results indicate that more accurate corrections by regression can be obtained over short intervals (< 20 seconds) which contain only correlated disturbances within the signal conditioning passband.

Single mode bias correction by multiple linear regression using the previously described frequency and time domain procedure was also applied to the modulated sine data sets for yaw excitation. Selected results are tabulated in Table 3 showing the time and duration of the corrected time series, the source of the integral-squared correction, the mean and standard deviation of the filtered uncorrected AOA, the bias error estimated by the regression, the mean of the corrected AOA, and the standard error of the regression.

Table 3
Estimated Bias Error with Yaw Excitation
(Unexcited Data Zero, AOA = -0.283°)

Record Segment (Sec)	Correction Source	Mean Filtered AOA (Deg)	Standard Deviation Filtered AOA (Deg)	Bias Estimate (Deg)	Mean Corrected AOA (Deg)	Standard Error (Deg)
10–30	Yaw	-0.433	0.078	-0.148	-0.285	0.007
40–60	Yaw	-0.440	0.077	-0.161	-0.280	0.032
10–30	Side	-0.433	0.078	-0.178	-0.254	0.050
10–30	Y Accel.	-0.433	0.078	-0.149	-0.284	0.021

Figure 26 illustrates the residuals of the AOA correction using integral-squared yaw computed over 10 to 30 seconds. Note that the AOA error after correction is reduced by 91 percent. In Table 3, the correction uncertainty increases tenfold in the 40 to 60 second interval because of a significant low frequency random disturbance in the integral-squared yaw which is absent in the AOA time series.

Optical System

The purpose of these tests was to determine the effect of dynamics on the video angle measurement method and compare with results for an onboard inertial sensor. For these dynamic tests the change in model AOA was of primary interest rather than the measurement of the AOA itself. In order to measure the error in indicated angle due to dynamics, it was necessary to determine the basic instrumentation repeatability. This repeatability was measured as the standard deviation of data recorded over time with the pitch angle fixed and could be classified as either short term (1 sec) or long term (several days).

The short-term repeatability for the video technique over 1 second (60 fields) was computed as the mean of the standard deviation at each of 36 "shaker off" data points and found to be 0.0018 ° with a maximum value of 0.0034 °. The mean standard deviation of the y-intercept for the "shaker off" points over 1 second was 0.0002 inch with a maximum value of 0.0006 inch.

The shaker was attached to the fuselage for measurements in yaw for the first 42 data points of the test, which occurred over a 48-hour period. Since the model pitch angle was assumed

unchanged during this period, the variability in the mean pitch angle measured for "shaker off" points characterizes the long-term repeatability of the angle measuring systems. The long-term repeatability was 0.0035 ° for the video technique and 0.0026 ° for the onboard accelerometer. If the pitch angle from the onboard accelerometer is subtracted from the video angle to account for small changes in angle over the 48-hour period, then the long-term repeatability of their difference is 0.0016°. This indicates that most of the increase in standard deviation compared to that found over 1 second was due to actual small pitch angle changes of the model during the 48 hours. During this time the standard deviation of the y-intercept variations was 0.0012 inch, indicating slight movement in the pitch plane between camera and model fuselage during the 48-hour test period.

The first point taken of each series of points, or run, was with the shaker off. The shaker load was then applied and additional points taken as the load was increased. The last point taken of each run was also a "shaker off" point. The mean of the angles measured at the start and end under no load was subtracted from each point of a given run and the "shaker off" points excluded from calculations so as not to bias the results. The standard deviation of the differences between the first and last pitch angles of the "shaker off" points was 0.0039° for the video technique and 0.0023° for the onboard accelerometer indicating good angle stability for the test.

Data were taken for 49 data points in dynamic yaw and 42 data points in dynamic pitch. Sine and modulated sine as well as random inputs from 5 to 60 Hz were used to drive the shaker to induce yawing and pitching moments of over 5000 inch-pounds peak-to-peak. For both the video technique and inertial (onboard accelerometer) technique, the mean of the first and last points with the shaker off was subtracted from the points with model dynamics induced by the shaker. A summary of all the data for yaw and pitch comparing the video technique with the inertial technique is shown in Table 4. In all cases the video pitch angle was determined from the mean of 60 angle recordings over 1 second.

Table 4
Summary of AOA Error for Video and Inertial AOA Measurements

Technique	Mean	Standard Deviation	Maximum	No. of Data Points	Excitation
Video	0.000°	0.002°	0.006°	49	Yaw
Inertial	-0.050°	0.057°	-0.217°	49	Yaw
Video	0.002°	0.004°	0.010°	42	Pitch
Inertial	-0.033°	0.046°	-0.174°	42	Pitch

Both the mean error and standard deviation of error for the video technique indicate very little additional error caused by the model dynamics whereas the onboard accelerometer suffers a large, generally negative, bias error that can be as large as 0.2 degrees. Summary plots of the AOA error in yaw and pitch for the video and inertial techniques are plotted versus peak-to-peak moment in figure 27. AOA errors for the various runs are plotted in figures 28–30. The dynamic yaw tests were conducted at several model pitch angles, whereas, the dynamic

pitch tests were limited to pitch angles near 0 degrees because of shaker mounting constraints.

Selected temporal variations over one second in the video measured angle during shaker excitation in yaw at 9.8 Hz are plotted in figure 31. The video technique recorded changes in pitch during yaw excitation of up to 0.04° at the largest yaw moment of almost 4000 in-lb peak-to-peak. The corresponding y-intercept plots are presented in figure 32 where displacements in the pitch plane of up to 0.01 inch are noted for the largest yaw moment. Example temporal angle variations over 4.6 sec during shaker excitation in pitch are plotted in figures 33 and 34 for 9.2 Hz sine excitation modulated at 0.25 Hz, and band-limited (5–60 Hz) random excitation. Pitch variations of almost 0.3 ° were noted during excitation of the 9.2 Hz pitch mode. The corresponding y-intercept plots are presented in figures 35 and 36 which show displacements in the pitch plane of up to 0.1 inch for the 9.2 Hz mode.

The standard deviation of the video measurements over 1 second versus yaw and pitch moment are presented in figure 37. The maximum standard deviation over 1 second for yaw moment is generally less that 0.02°, even for the largest moments, indicating very little dynamic pitching during yaw dynamics. The maximum value for the largest pitch moment is 10 times larger due to the dynamic changes in pitch angle during dynamic pitch.

Concluding Remarks

Servo-accelerometers are excellent devices and widely used for measuring angle of attack for wind-tunnel models. However, when these inertial devices are used in the presence of significant model system vibrations, bias errors are introduced due to centrifugal accelerations associated with model system oscillations. This bias error can be difficult to estimate and correct. An experimental study of inertial and optical model attitude measurement systems response in a wind-off dynamic environment is presented in this paper. This study is a benchmark test for developing new model attitude measurement systems as well as studying techniques for correcting existing inertial sensors in order to obtain high accuracy angle of attack measurements in a hostile dynamic environment. The results of this study will be used for evaluating model attitude measurements using the inertial and optical systems during wind-tunnel tests of the model system testbed. Further work needs to be done to extend the AOA correction algorithms to multiple mode excitation/response and validate the algorithms during actual wind-tunnel tests.

The modal correction technique developed and used for calculating the AOA bias error worked very well for the wind-off dynamic environment of sinusoidal, modulated sinusoidal, and random forced response testing. It was found that some of the model system vibration modes excited to high levels during wind-tunnel tests in the NTF could not be excited very well in the NTF model assembly bay. This is attributed to boundary conditions at the assembly bay model support which are quite different from the NTF model support system. This points out the need for doing modal testing on the model system after installation in the tunnel to assure the most accurate measurement of the vibration mode radii and for the evaluation of the AOA response to model system vibrations.

The frequency and time domain bias correction technique proved to be a reliable means of detecting normal acceleration components due to modulated angular acceleration in the pitch and yaw plane. The cross-spectral coherence function detects the presence of low frequency normal acceleration components in AOA which are correlated with the integral-squared angular acceleration in pitch and yaw. These components can be removed from the AOA time series by subtracting a weighted, filtered portion of the integral-squared yaw (or pitch) time series. However, the presence of uncorrelated spectral content below the correlated spectral components produces residual errors in the corrected result which limit the amount of correction available.

The optical system employing a single video camera gave excellent results in the assembly bay tests. The mean pitch angle of 60 recordings over 1 second determined by the video method does not appear to be adversely affected by dynamics in yaw or pitch. However, it should be noted that this test concentrated on dynamic effects and that more tests are needed to ascertain the video method's instrumental uncertainty, reliability, and applicability to the measurement of model pitch angle with flow and at various conditions in both conventional and cryogenic wind-tunnels. Performance tests of this system during actual wind-tunnel operation are underway.

References

1. Finley, T. and Tcheng, P.: Model Attitude Measurements at NASA Langley Research Center. AIAA-92-0763, 1992.

2. Fuller, D. E.: Guide to Users of the National Transonic Facility. NASA TM-83124, July 1981.

3. Strganac, T. W.: A Study of the Aeroelastic Stability for the Model Support System of the National Transonic Facility. AIAA-88-2033, 1988.

4. Whitlow, W., Jr.; Bennet, R. M.; and Strganac, T. W.: Analysis of Vibrations of the National Transonic Facility Model Support System Using a 3-D Aeroelastic Code. AIAA-89-2207, 1989.

5. Young, C. P., Jr.; Popernack, T. G., Jr.; and Gloss, B. B.: National Transonic Facility Model and Model Support Vibration Problems. AIAA-90-1416, 1990.

6. Buehrle, R. D.; Young, C. P., Jr.; Balakrishna, S.; and Kilgore, W. A.: Experimental Study of Dynamic Interaction Between Model Support Structure and a High Speed Research Model in the National Transonic Facility. AIAA-94-1623, 1994.

7. Young, C. P., Jr.; Buehrle, R. D.; Balakrishna, S.; and Kilgore, W. A.: Effects of Vibration on Inertial Wind-Tunnel Model Attitude Measurement Devices. NASA TM-109083, August 1994.

8. Pond, C. R. and Texeira, P. D.: Laser Angle Sensor Development. NASA CR-159385, Oct. 1980.

9. Crites, R. C.: Development of a Simple Optical Pitch Sensor. AIAA-86-0770.

10. Owen, F. K.: An Optical Angle-of-Attack Sensor. SBIR Contract NAS2-13202, 1987.

11. Schott, T. and Tcheng, P.: An Electro-optical Wind-tunnel Model Position Detector. 37th ISA, vol. 37, pp. 147-161, May 1991.

12. Burner, A. W.; Snow, W. L.; Shortis, M. R.; and Goad, W. K.: Laboratory Calibration and Characterization of Video Cameras. presented at ISPRS Symposium: Close-Range Photogrammetry Meets Machine Vision, Zurich, Switzerland, Sept. 1990; published in SPIE Proceedings 1395, pp. 664-671.

13. Shortis, M. R.; Burner, A. W.; Snow, W. L.; and Goad, W. K.: Calibration Tests of Industrial and Scientific CCD Cameras. Invited paper presented at First Australian Photogrammetry Conference, Sydney, Nov. 7-9, Paper 6, 11 pages, 1991.

14. MATLAB Reference Guide, The Math Works Inc., August, 1992.

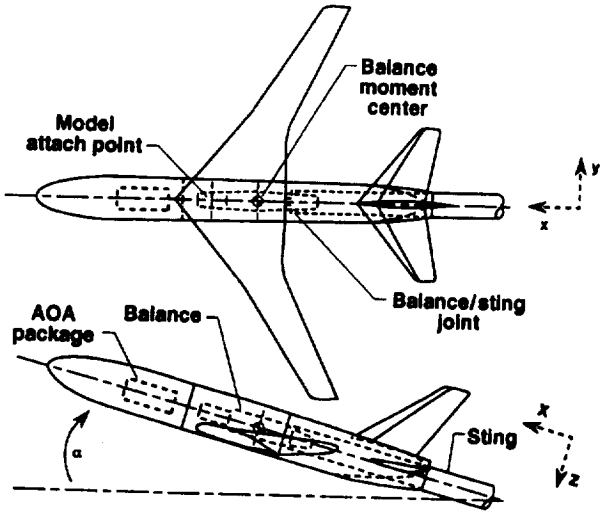

Figure 1.- Schematic of wind tunnel model system.

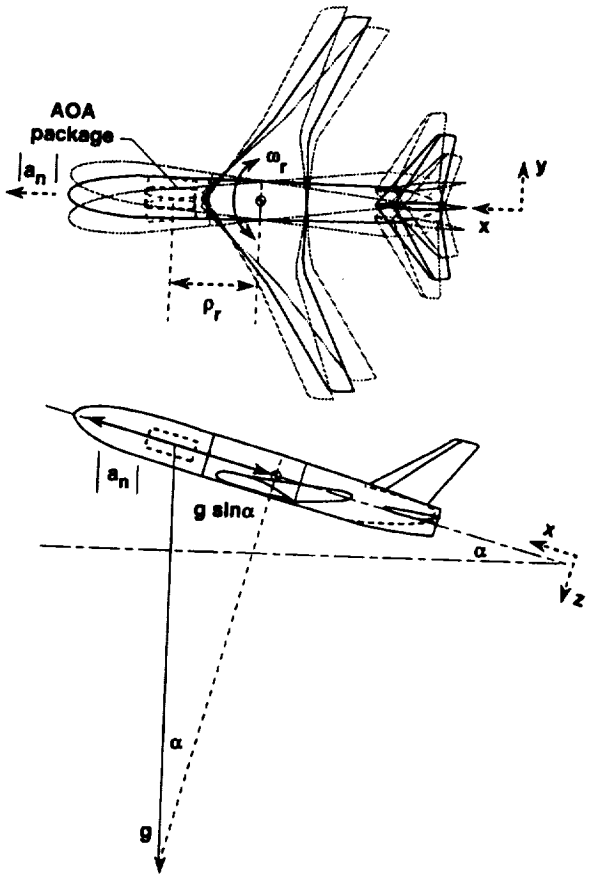

Figure 2.- Effect of vibration on inertial model attitude measurement.

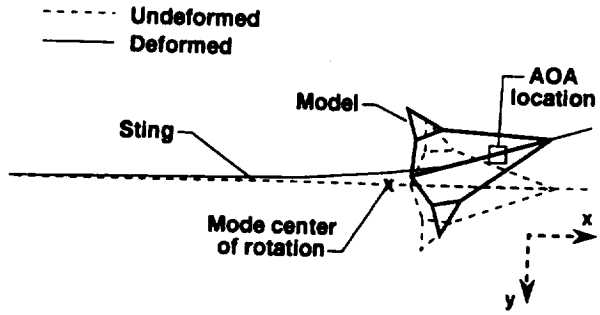

Figure 3.- Sting bending in yaw plane, 9.0 Hz vibration mode.

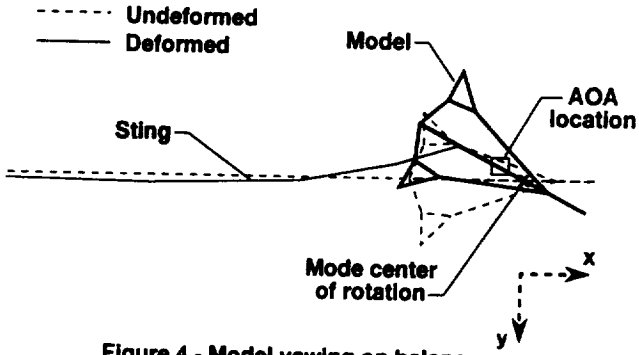

Figure 4.- Model yawing on balance, 29.8 Hz vibration mode.

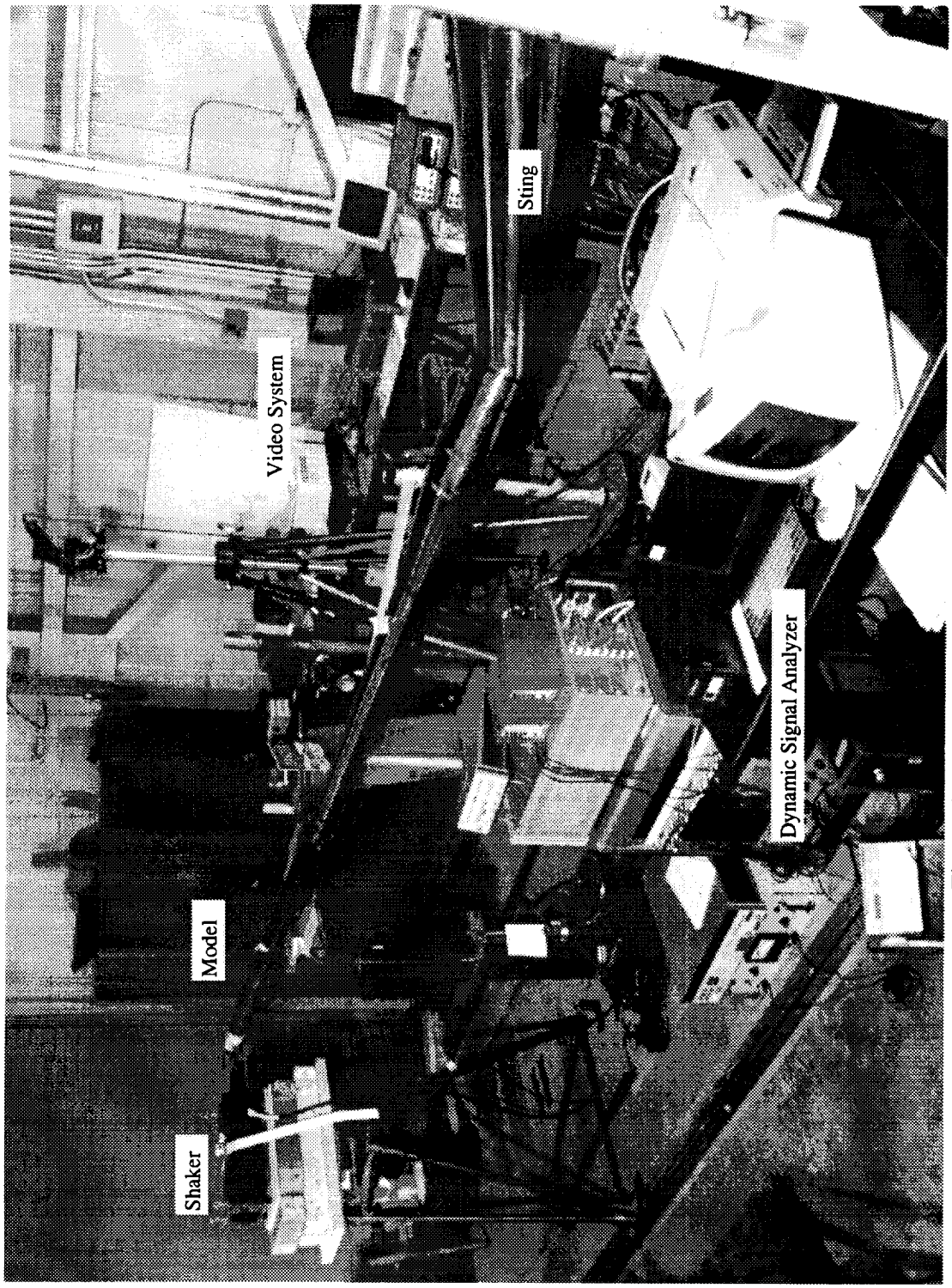

Figure 5. Test setup in model assembly bay.

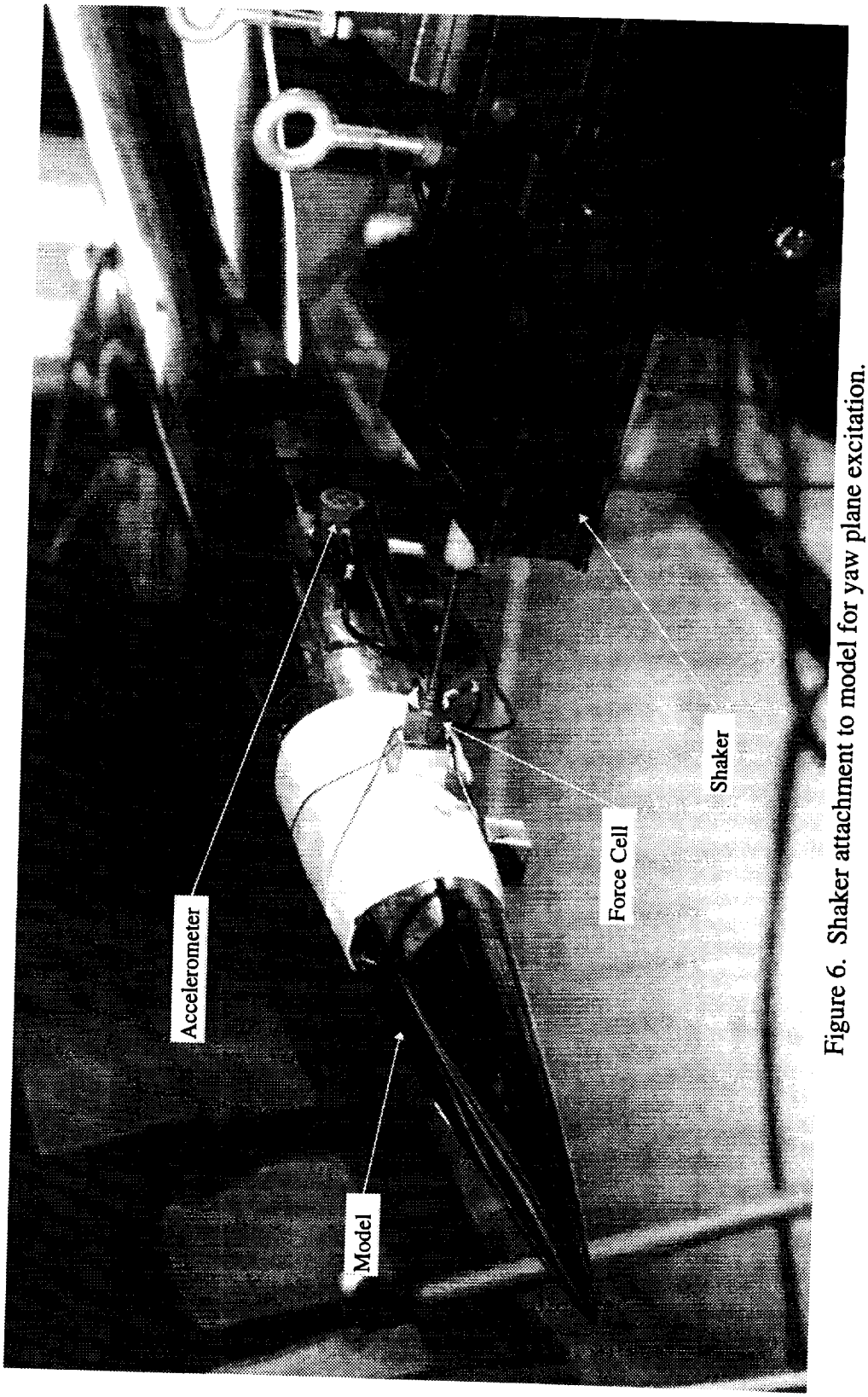

Figure 6. Shaker attachment to model for yaw plane excitation.

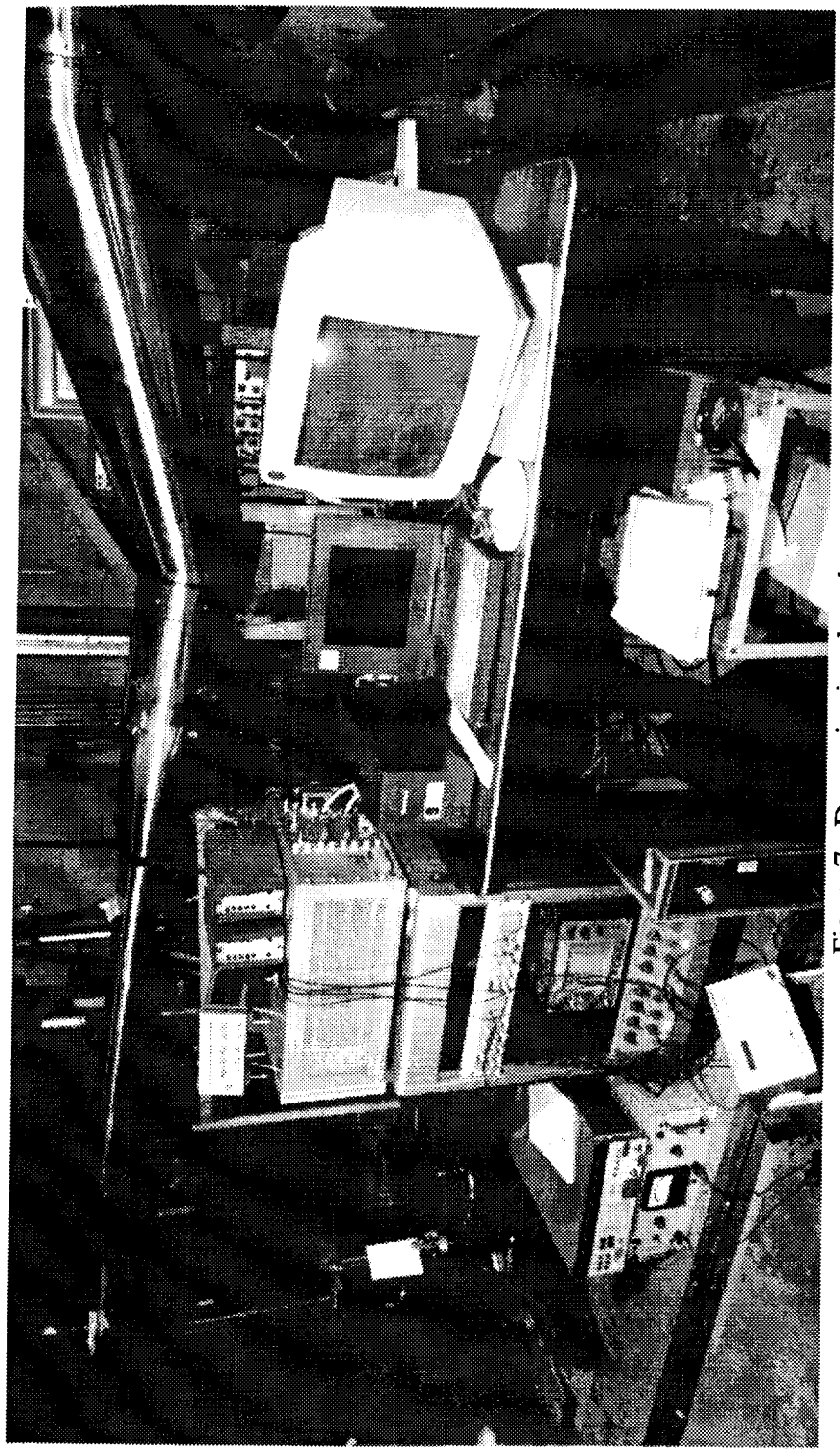

Figure 7. Dynamic signal analyzer.

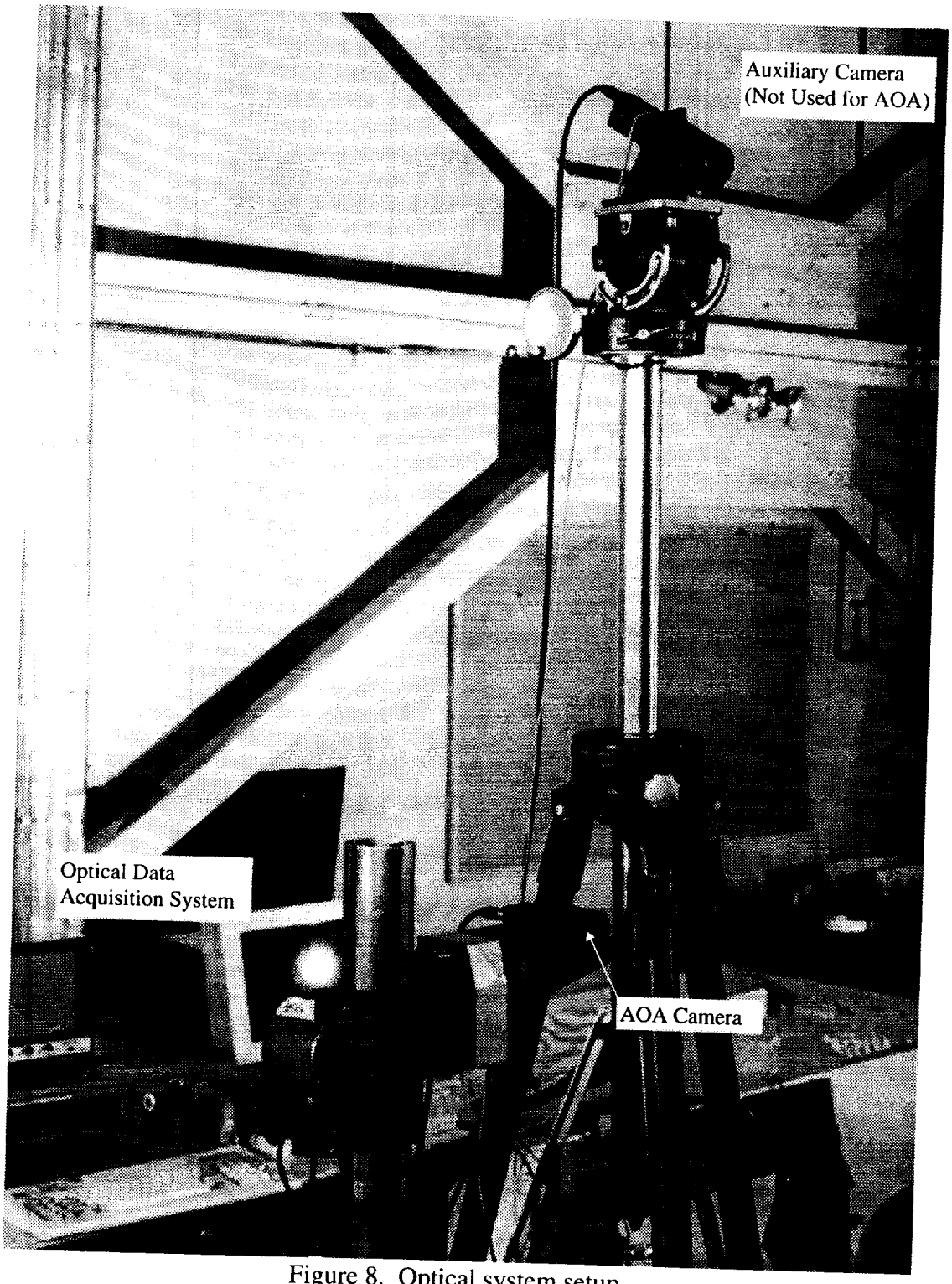

Figure 8. Optical system setup.

Figure 9. Video/Optical system data acquisition equipment.

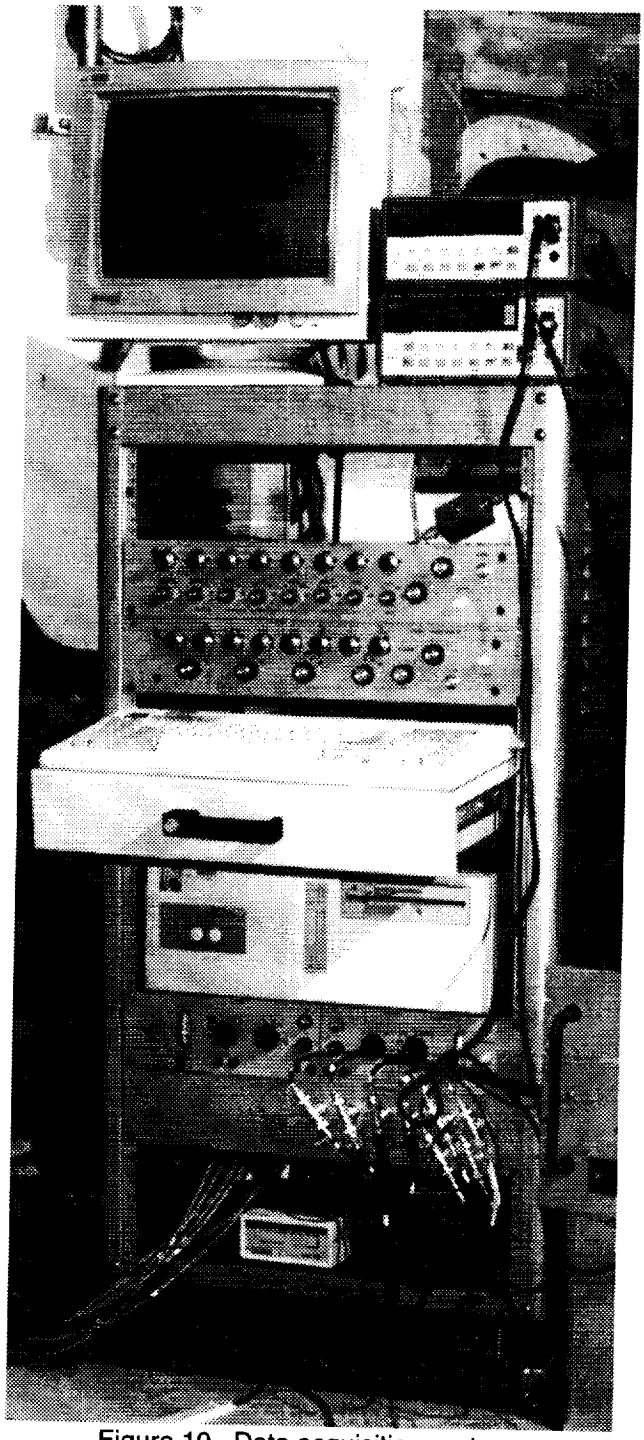

Figure 10. Data acquisition system.

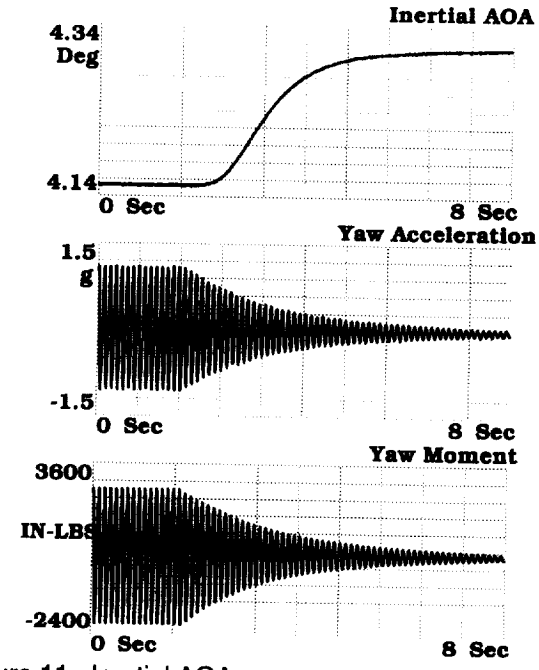

Figure 11. Inertial AOA measurement, yaw acceleration, and yaw moment versus time for 9.0 Hz sinusoidal input in yaw plane.

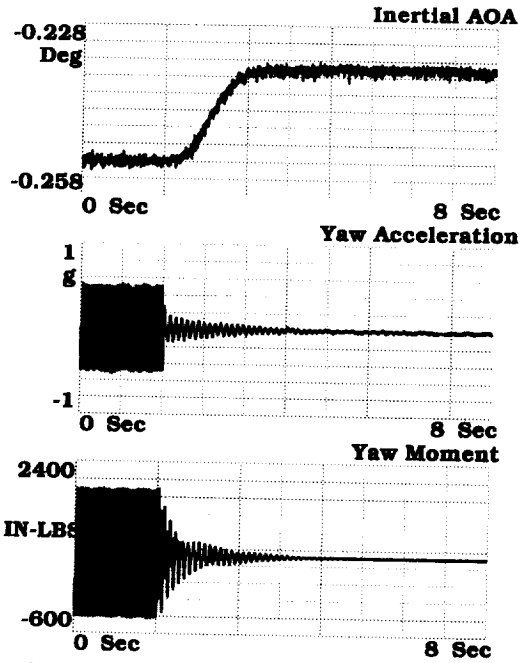

Figure 12. Inertial AOA measurement, yaw acceleration, and yaw moment versus time for 19.5 Hz sinusoidal input in yaw plane.

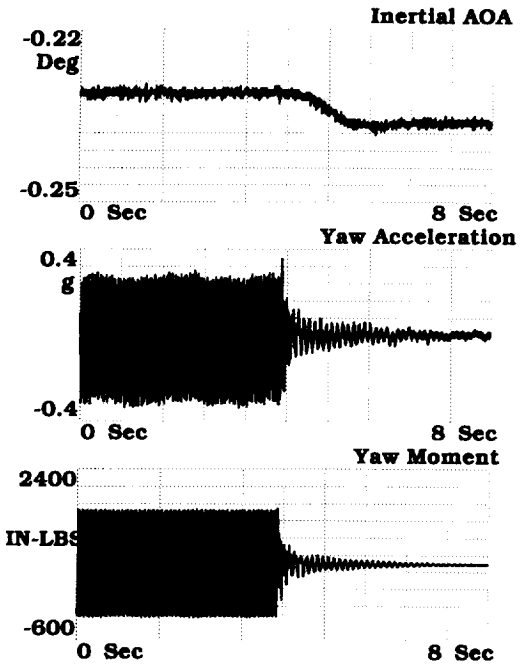

Figure 13. Inertial AOA measurement, yaw acceleration, and yaw moment versus time for 29.8 Hz sinusoidal input in yaw plane.

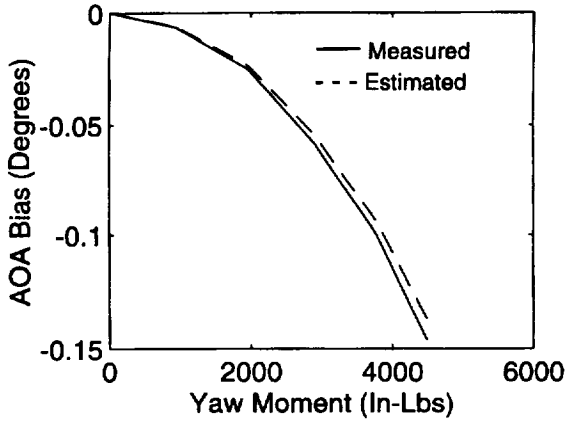

Figure 14. Measured and estimated AOA bias error versus peak-to-peak yaw moment for 9.0 Hz yaw mode.

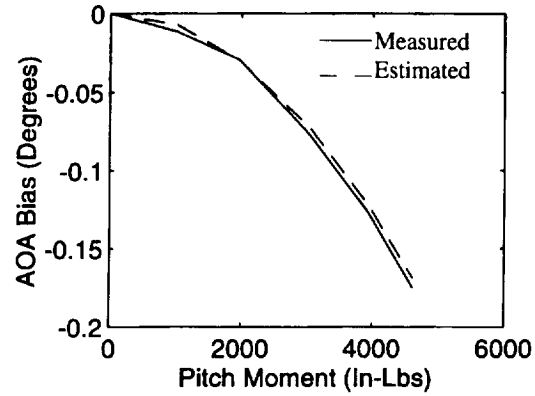

Figure 15. Measured and estimated AOA bias error versus peak-to-peak pitch moment for 9.2 Hz pitch mode.

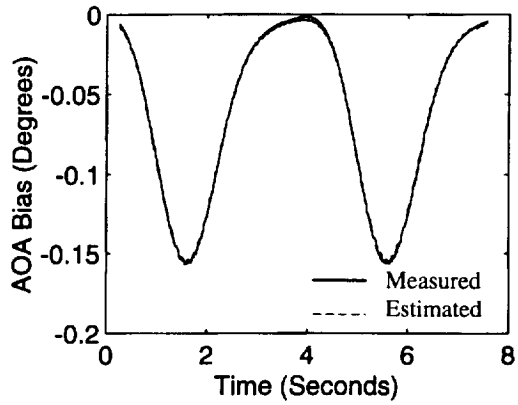

Figure 16. Measured and estimated AOA bias error versus time for 9.2 Hz sinusoidal excitation in pitch with 0.25 Hz modulation, maximum peak-to-peak pitch moment of 4500 inch-pounds.

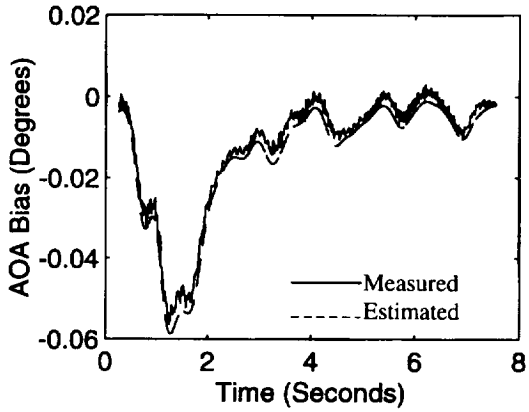

Figure 17. Measured and estimated AOA bias error versus time for random excitation in pitch.

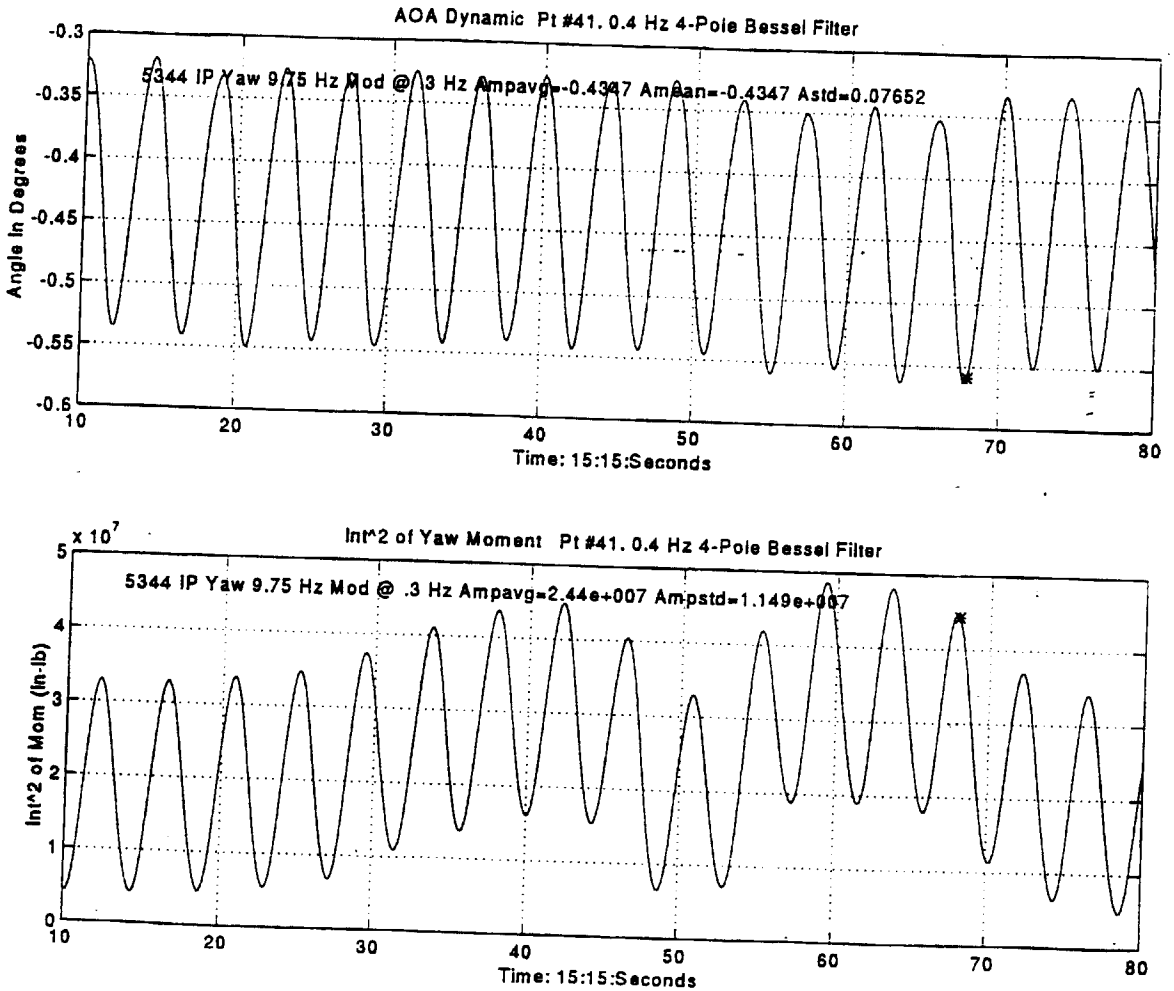

Figure 18. Filtered AOA output and integral-squared yawing moment for yaw excitation of 5300 inch-pounds at 9.75 Hz with 0.3 Hz modulation.

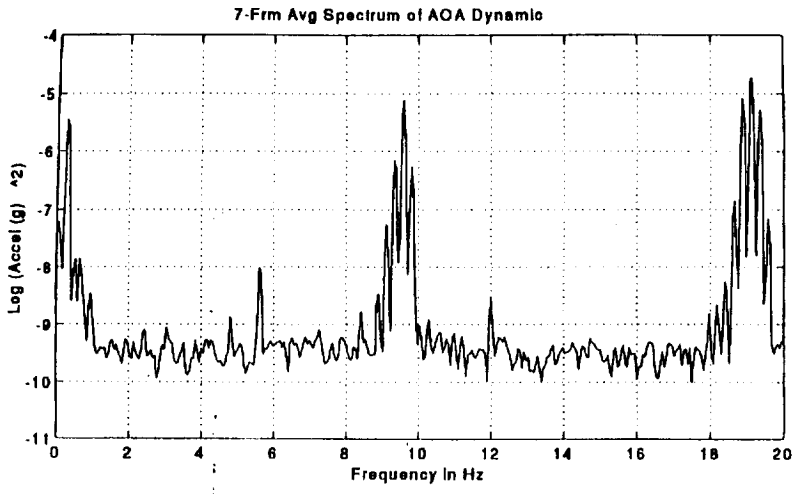

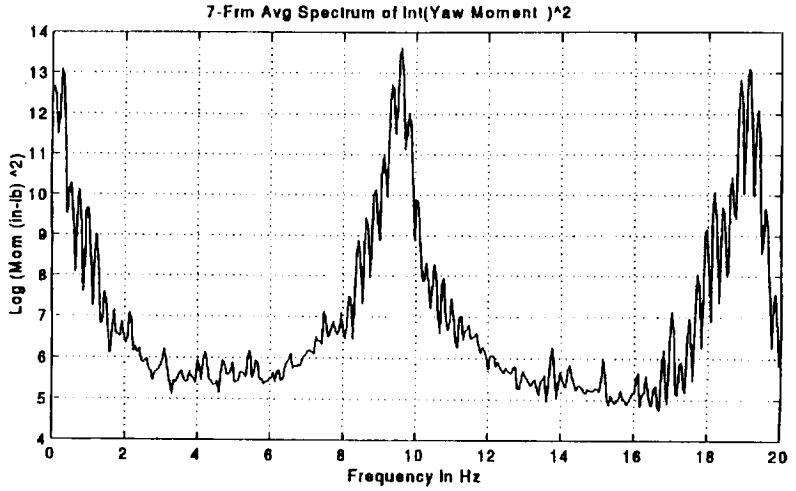

Figure 19. Power spectra of AOA output and integral-squared yawing moment for yaw excitation of 5300 inch-pounds at 9.75 Hz with 0.3 Hz modulation.

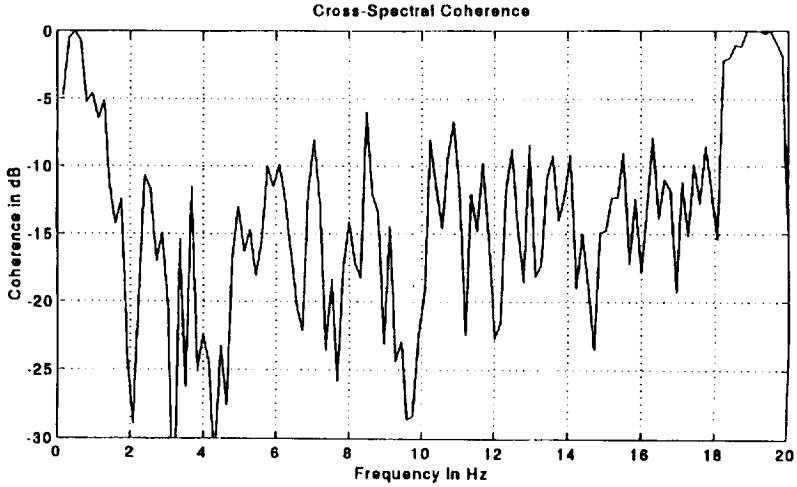

Figure 20. Cross-spectral coherence between AOA output and integral-squared yawing moment for yaw excitation of 5300 inch-pounds at 9.75 Hz with 0.3 Hz modulation.

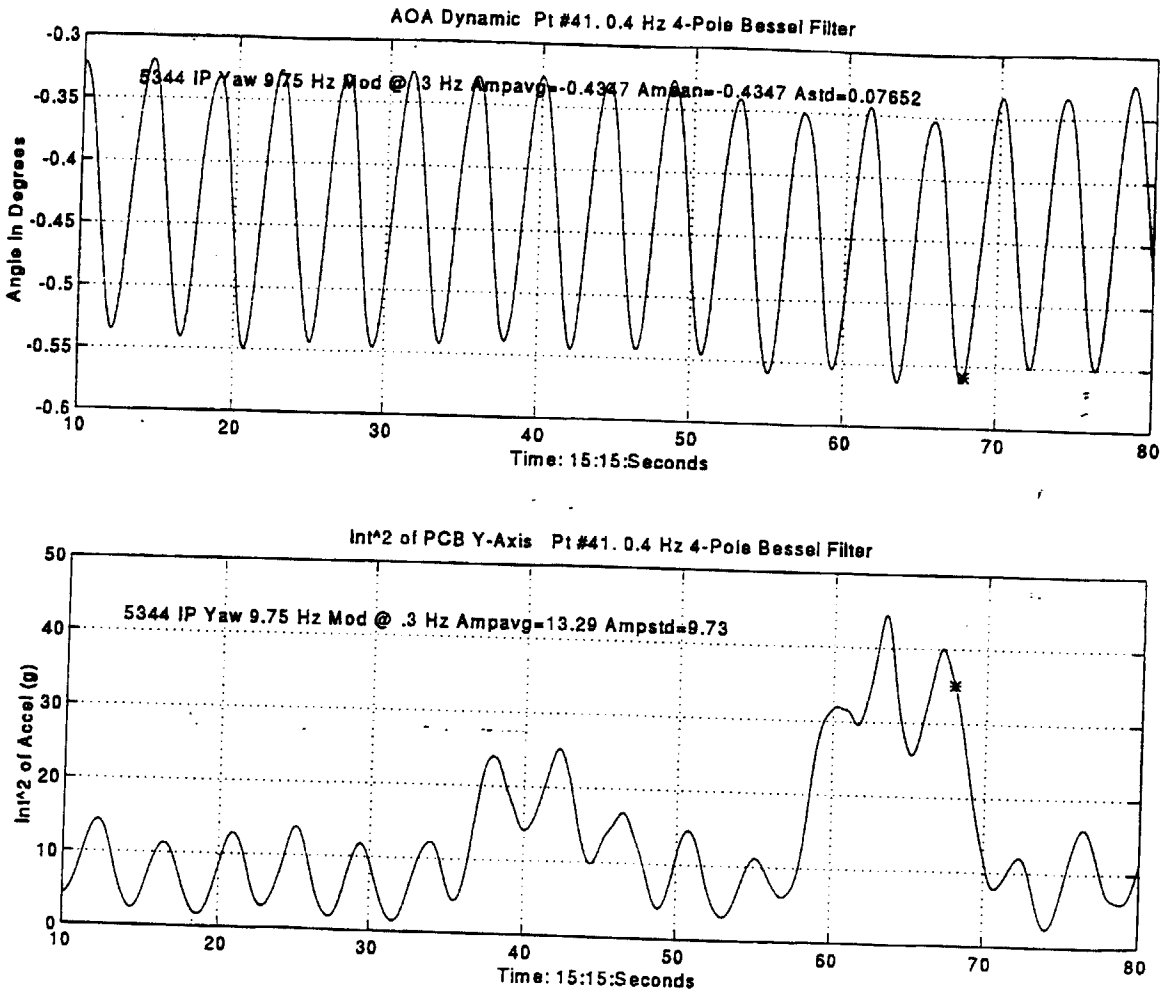

Figure 21. Filtered AOA output and integral-squared y-axis acceleration for yaw excitation of 5300 inch-pounds at 9.75 Hz with 0.3 Hz modulation.

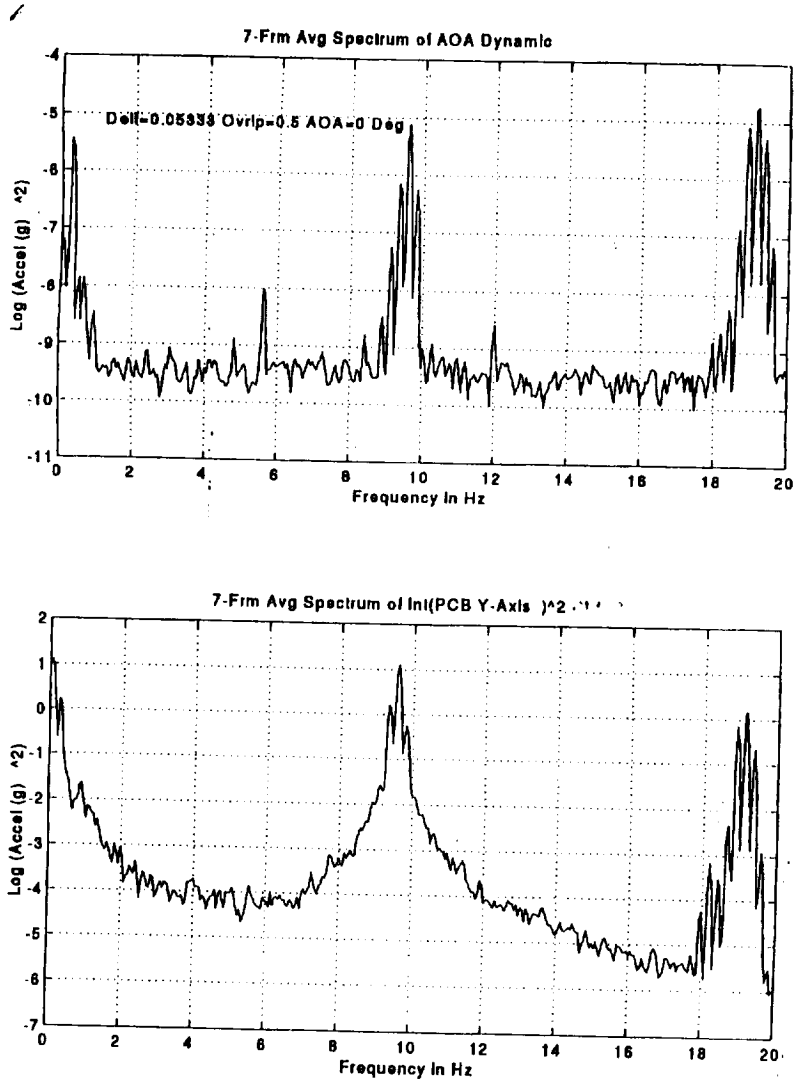

Figure 22. Power spectra of AOA output and integral-squared y-axis acceleration for yaw excitation of 5300 inch-pounds at 9.75 Hz with 0.3 Hz modulation.

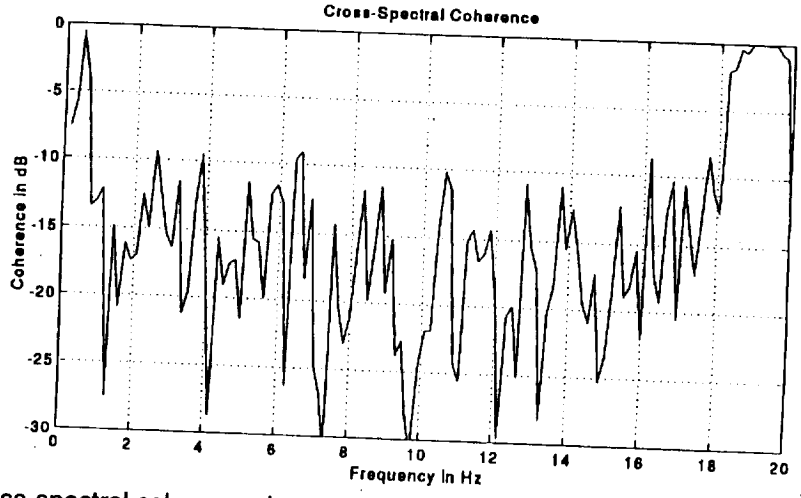

Figure 23. Cross-spectral coherence between AOA output and integral-squared y-axis acceleration for yaw excitation of 5300 inch-pounds at 9.75 Hz with 0.3 Hz modulation.

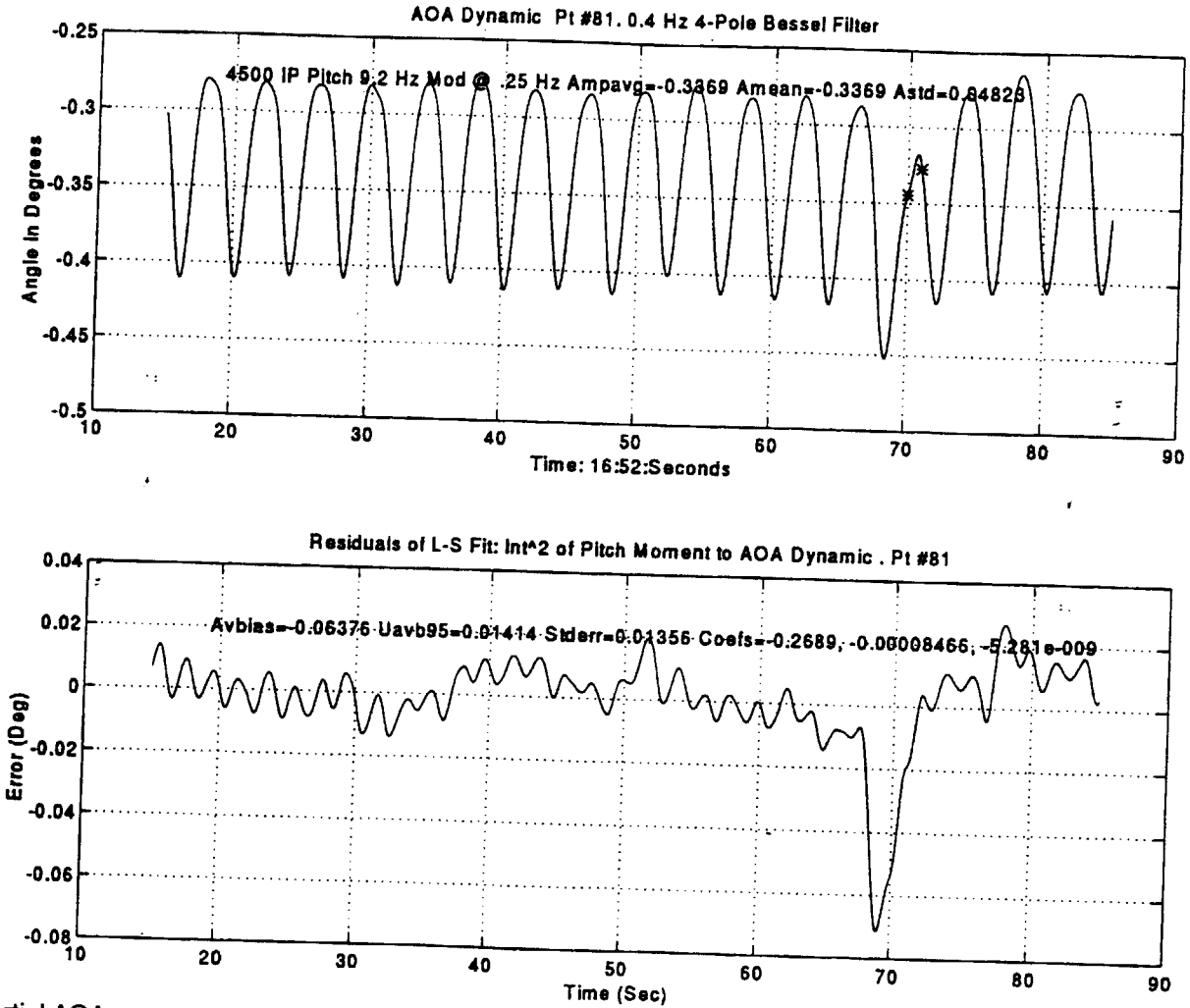

Figure 24. Inertial AOA measurement and residual of AOA correction using integral-squared pitch moment over a 15 to 85 second interval for 9.2 Hz sine input with 0.25 Hz modulation in pitch plane.

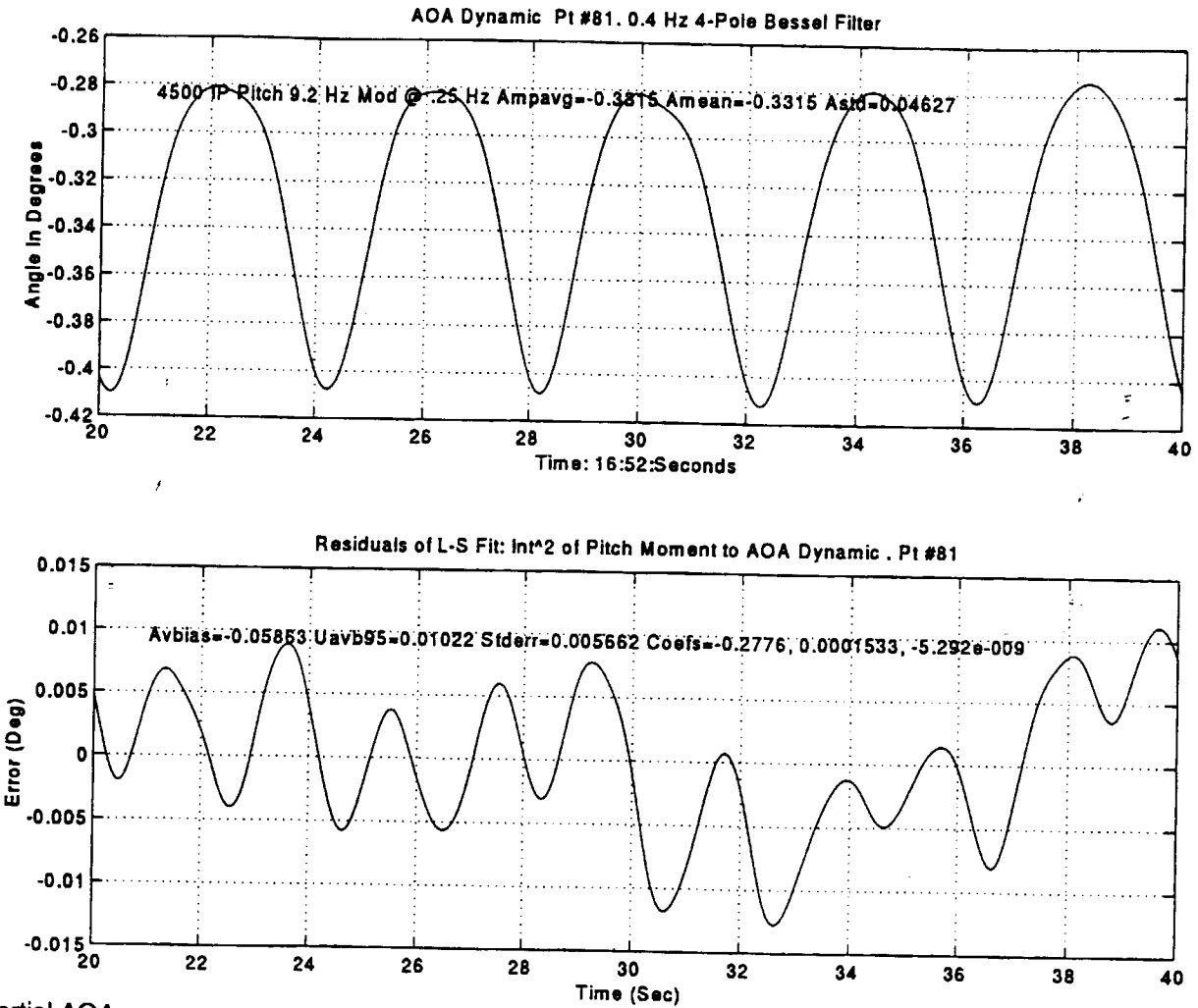

Figure 25. Inertial AOA measurement and residual of AOA correction using integral-squared pitch moment over a 20 to 40 second interval for 9.2 Hz sine input with 0.25 Hz modulation in pitch plane.

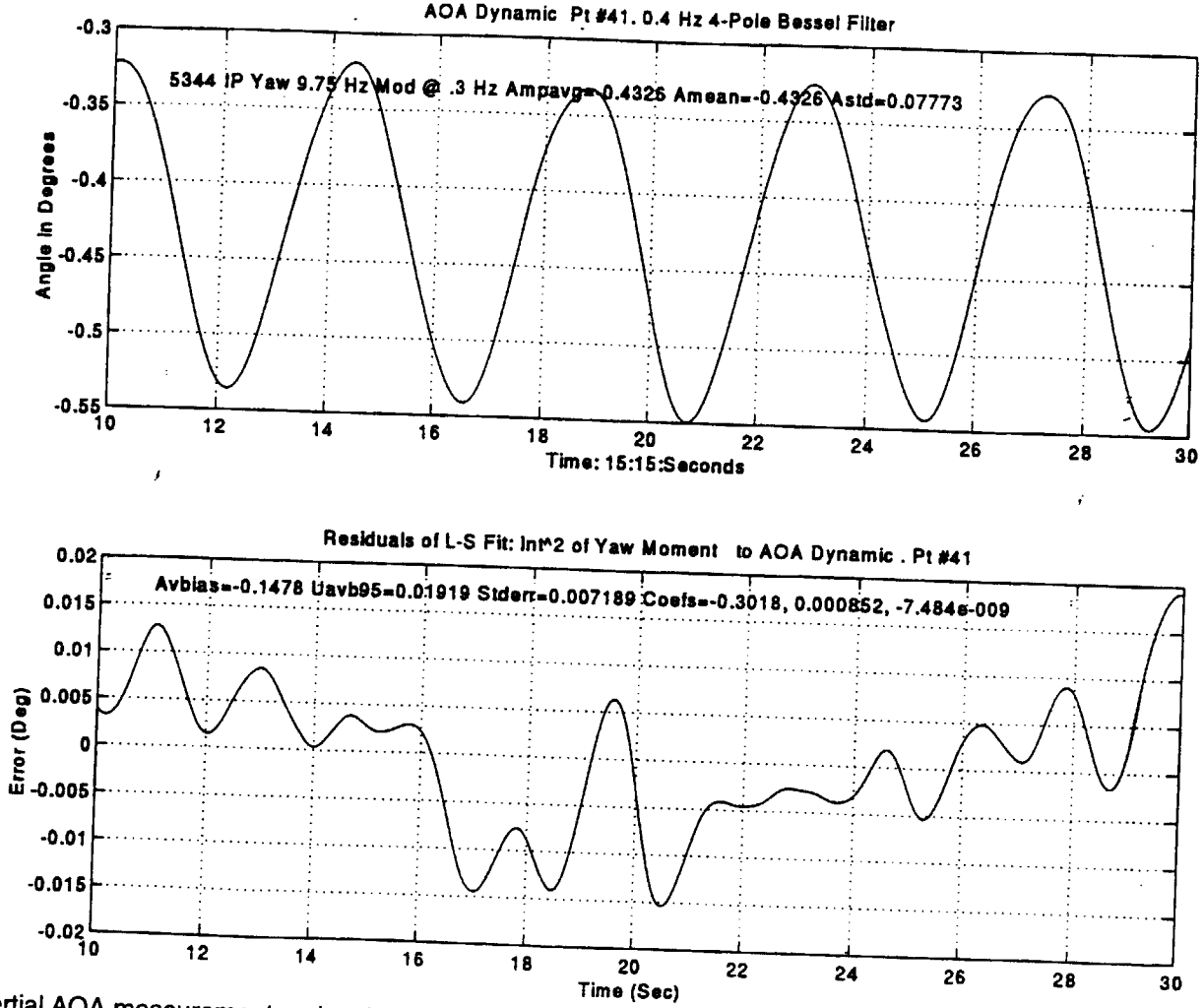

Figure 26. Inertial AOA measurement and residual of AOA correction using integral-squared yaw moment over a 10 to 30 second interval for 9.75 Hz sine input with 0.3 Hz modulation in yaw plane.

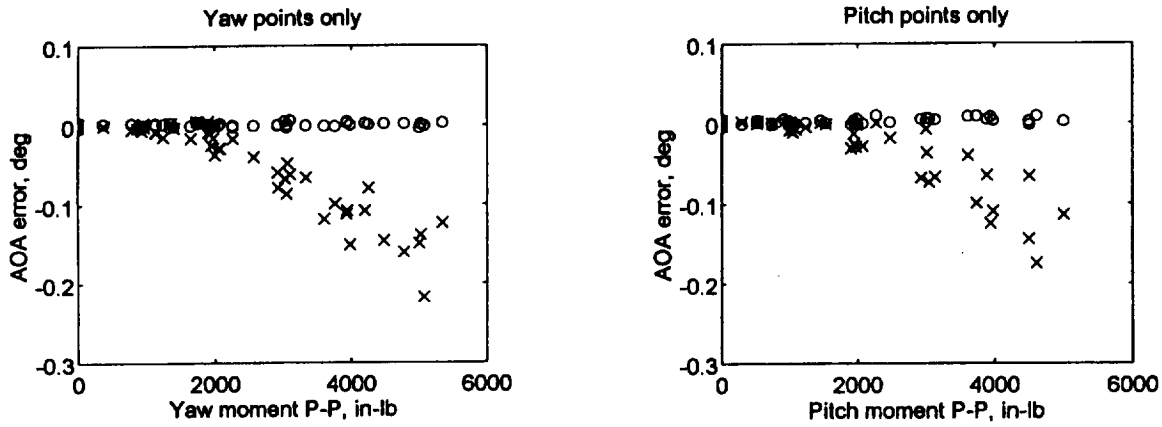

Figure 27. Indicated AOA bias errror versus peak-to-peak moment for video method (denoted with circles) and onboard inertial AOA device (denoted with X's) for all yaw and pitch tests.

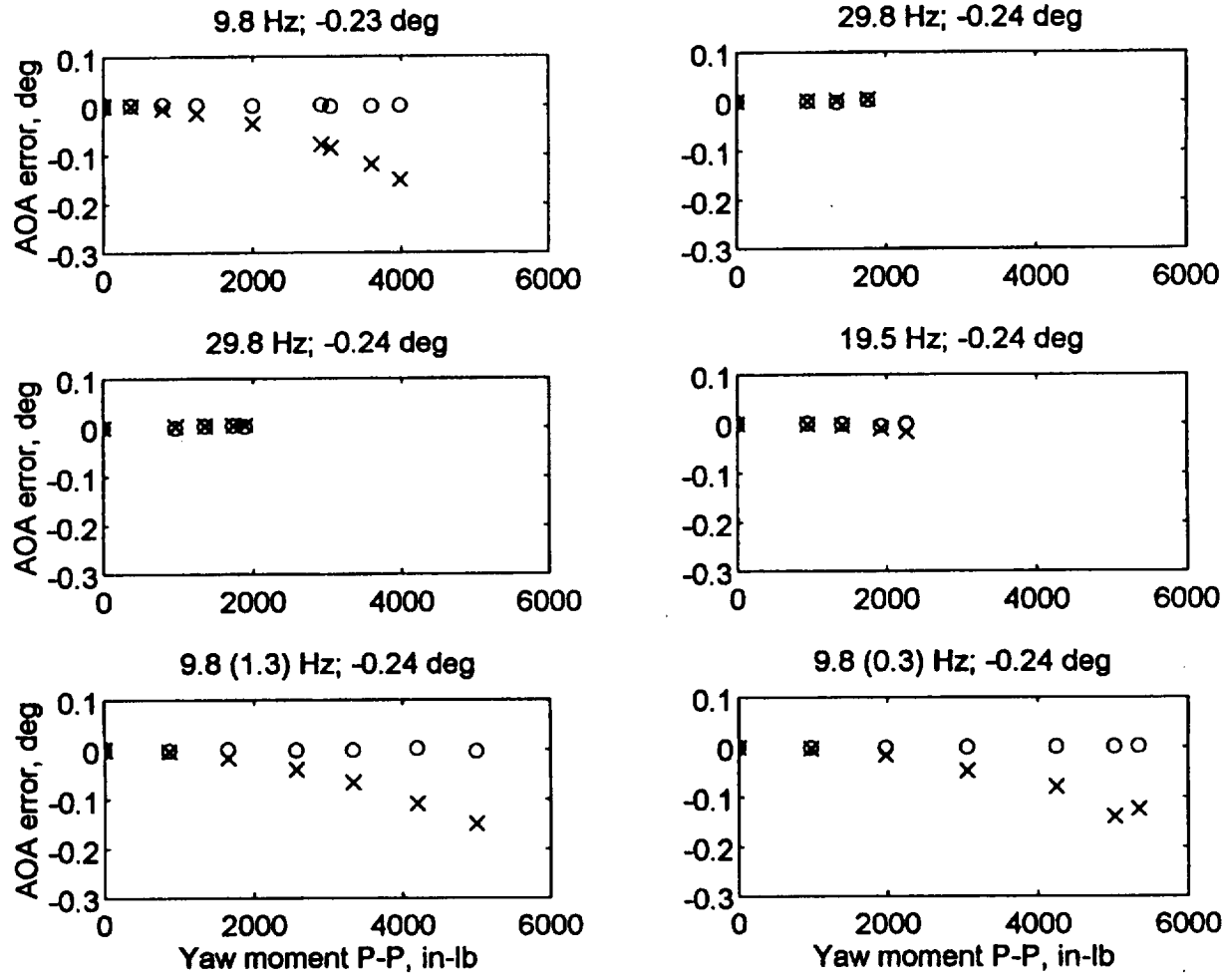

Figure 28. Comparison of AOA bias error versus peak-to-peak yaw moment for video method (denoted with circles) and onboard inertial AOA device (denoted with X's) with the excitation frequency, modulation frequency (in parantheses where appropriate), and nominal angle identified at the top of each plot.

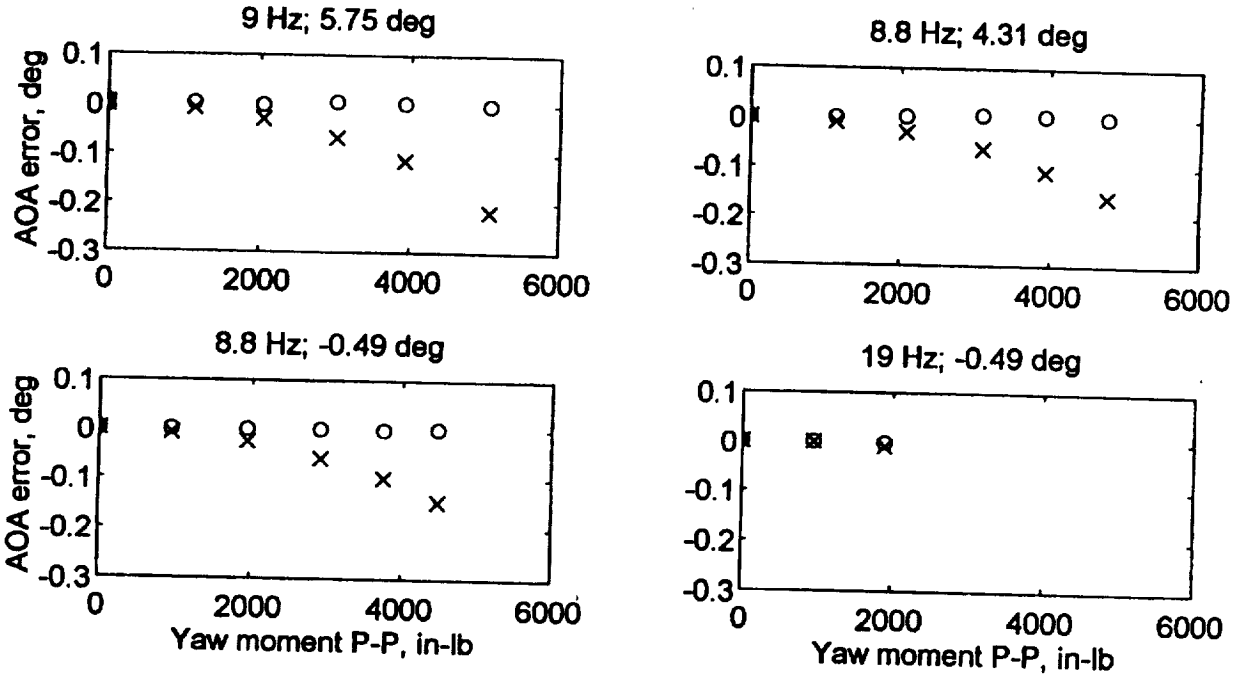

Figure 29. Comparison of AOA bias error versus peak-to-peak yaw moment for video method (denoted with circles) and onboard inertial AOA device (denoted with X's) with the excitation frequency and nominal angle identified at the top of each plot.

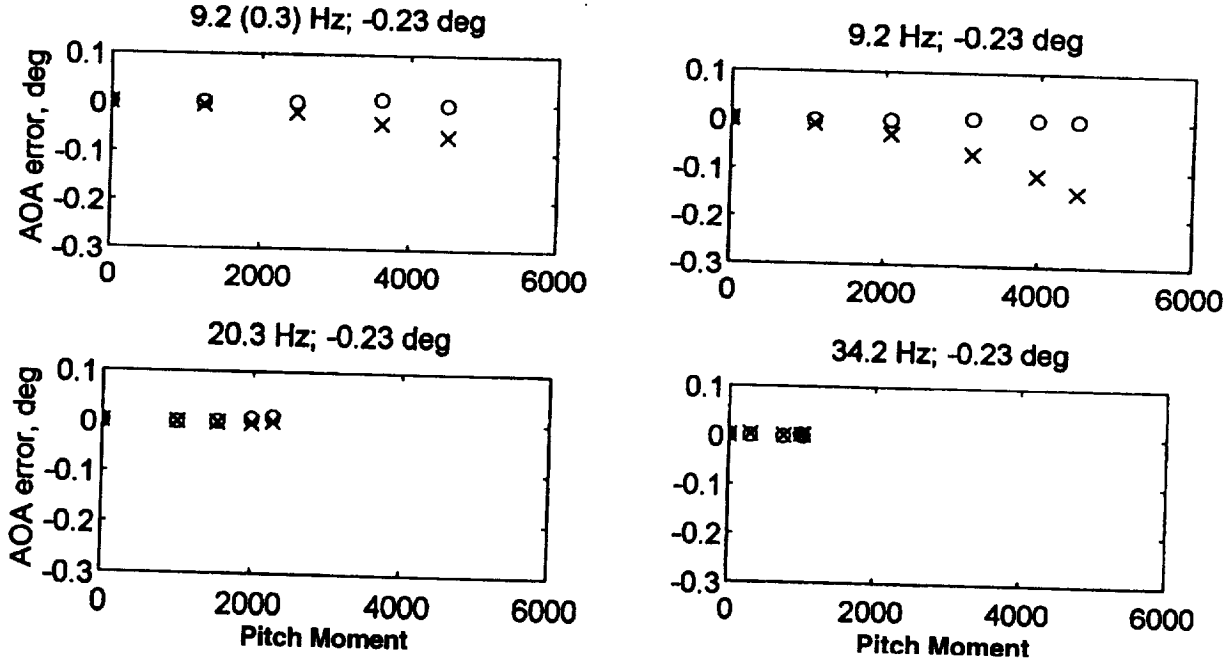

Figure 30. Comparison of AOA bias error versus peak-to-peak pitch moment for video method (denoted with circles) and onboard inertial AOA device (denoted with X's) with the excitation frequency, modulation frequency (in paranthese where appropriate), and nominal angle identified at the top of each plot.

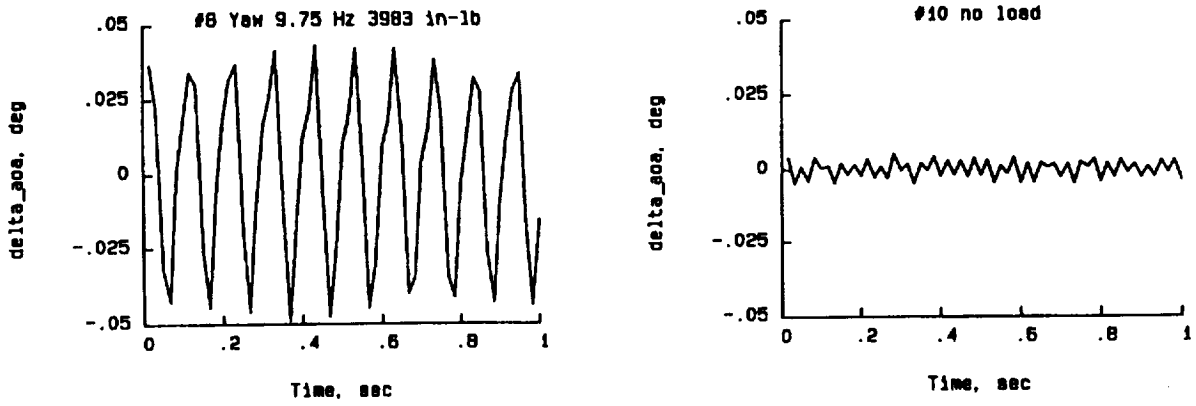

Figure 31. Change in pitch angle versus time measured with the video method for 9.75 Hz yaw excitation at yaw moments of 3983 in-lbs and zero.

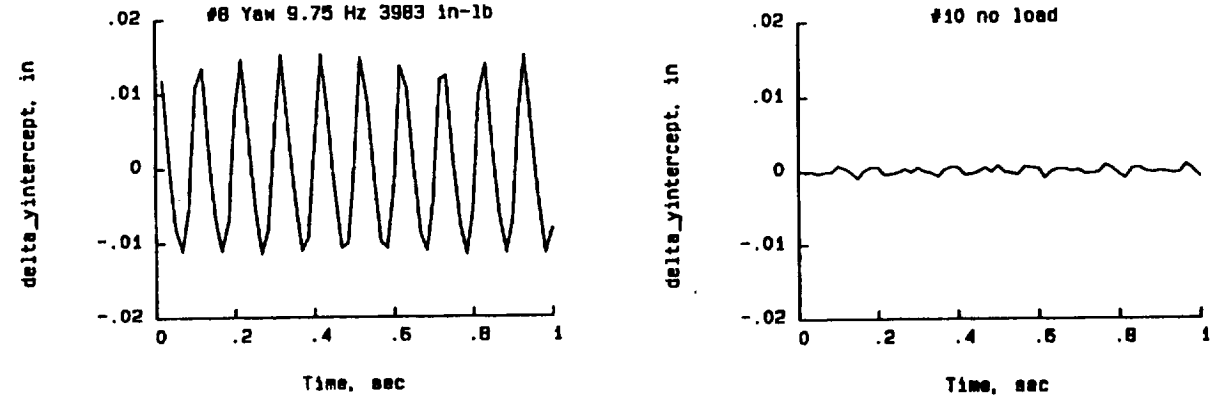

Figure 32. Corresponding change in Y-intercept versus time as measured with the video method for the same measurement points as Figure 31.

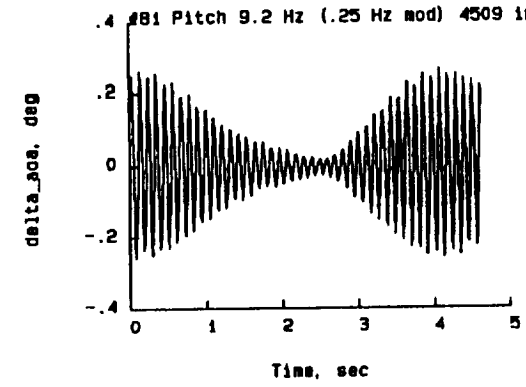

Figure 33. Change in pitch angle versus time measured woith the video method for 9.2 Hz pitch excitation with 0.25 Hz modulation and a maximum peak-to-peak pitch moment of 4509 in-lbs.

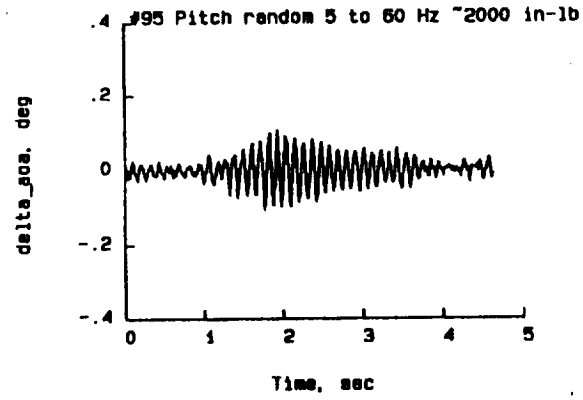

Figure 34. Change in pitch angle versus time measured with the video method for 5-60 Hz random excitation in pitch plane.

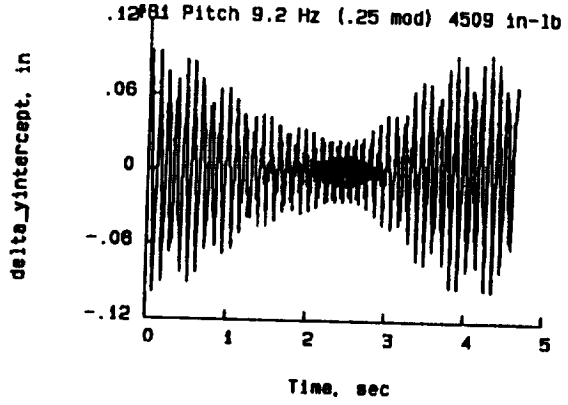

Figure 35. Corresponding change in Y-intercept versus time as measured with the video method for the same measurement point as Figure 33.

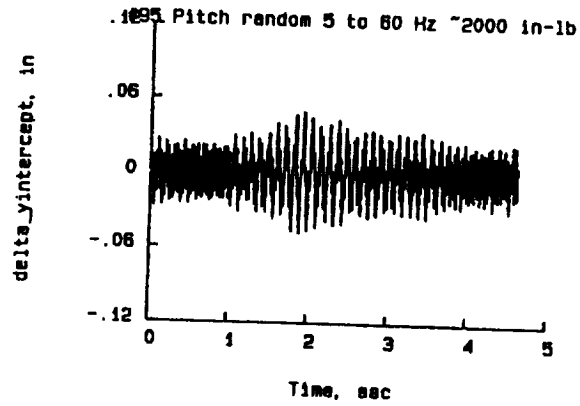

Figure 36. Corresponding change in Y-intercept versus time as measured with the video method for the same measurement point as Figure 34.

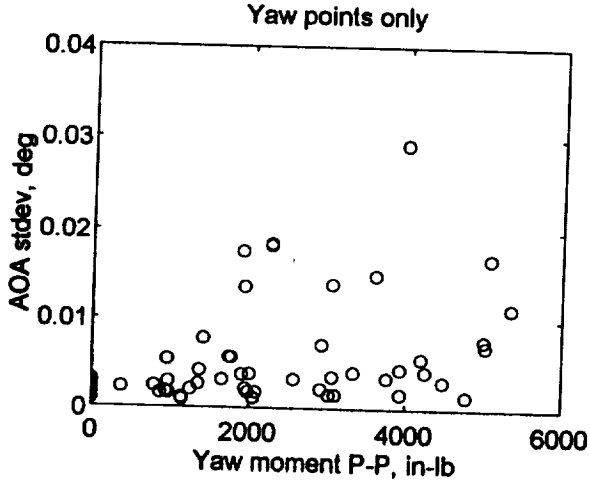

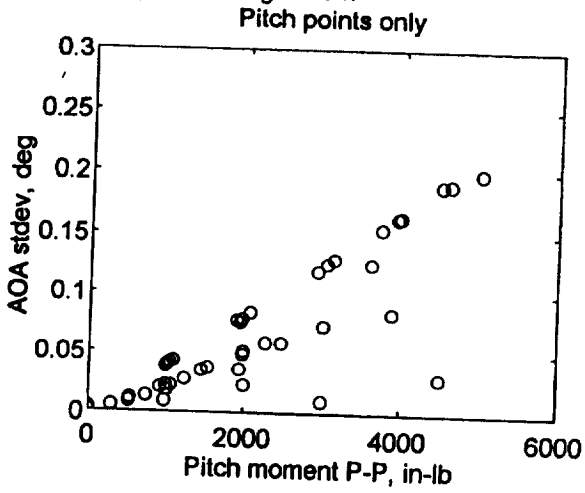

Figure 37. Video method pitch angle standard deviation over one second versus peak-to-peak yaw and pitch moment of the model.

REPORT DOCUMENTATION PAGE

Form Approved
OMB No. 0704-0188

1. AGENCY USE ONLY (*Leave blank*)	2. REPORT DATE	3. REPORT TYPE AND DATES COVERED
	February 1995	Technical Memorandum

4. TITLE AND SUBTITLE
Dynamic Response Tests of Inertial and Optical Wind-Tunnel Model Attitude Measurement Devices

5. FUNDING NUMBERS
WU 505-59-54-01

6. AUTHOR(S)
R. D. Buehrle, C. P. Young, Jr., A. W. Burner, J. S. Tripp, P. Tcheng, T. D. Finley, and T. G. Popernack, Jr.

7. PERFORMING ORGANIZATION NAME(S) AND ADDRESS(ES)
NASA Langley Research Center
Hampton, VA 23681-001

8. PERFORMING ORGANIZATION REPORT NUMBER

9. SPONSORING / MONITORING AGENCY NAME(S) AND ADDRESS(ES)
National Aeronautics and Space Administration
Washgton, DC 20546-0001

10. SPONSORING / MONITORING AGENCY REPORT NUMBER
NASA TM-109182

11. SUPPLEMENTARY NOTES
Buehrle, Burner, Tripp, Tcheng, Finley, Popernack: Langley Research Center, Hampton, VA
Young: North Caroline State University, Raleigh, N.C.

12a. DISTRIBUTION / AVAILABILITY STATEMENT
Unclassified - Unlimited

Subject Category 09

12b. DISTRIBUTION CODE

13. ABSTRACT (*Maximum 200 words*)

Results are presented for an experimental study of the response of inertial and optical wind-tunnel model attitude measurement systems in a wind-off simulated dynamic environment. This study is part of an ongoing activity at the NASA Langley Research Center to develop high accuracy, advanced model attitude measurement systems that can be used in a dynamic wind-tunnel environment. This activity was prompted by the inertial model attitude sensor response observed during high levels of model vibration which results in a model attitude measurement bias error. Significant bias errors in model attitude measurement were found for the measurement using the inertial device during wind-off dynamic testing of a model system. The amount of bias present during wind-tunnel tests will depend on the amplitudes of the model dynamic response and the modal characteristics of the model system. Correction models are presented that predict the vibration-induced bias errors to a high degree of accuracy for the vibration modes characterized in the simulated dynamic environment. The optical system results were uncorrupted by model vibration in the laboratory setup.

14. SUBJECT TERMS
Model Attitude Measurement; Wind Tunnel; Model Vibration; and Bias Error

15. NUMBER OF PAGES
43

16. PRICE CODE
A03

17. SECURITY CLASSIFICATION OF REPORT	18. SECURITY CLASSIFICATION OF THIS PAGE	19. SECURITY CLASSIFICATION OF ABSTRACT	20. LIMITATION OF ABSTRACT
Unclassified	Unclassified		